

A Real-Space Refinement Procedure for Proteins

BY R. DIAMOND

Medical Research Council Laboratory of Molecular Biology, Hills Road, Cambridge, England

(Received 23 March 1970 and in revised form 17 June 1970)

This paper describes a procedure which optimizes the fitting of a 'model' of a protein to an electron density map. The technique seeks to minimize $\int (\rho_o - \rho_m)^2 dv$ where ρ_o is the observed electron density and ρ_m is a density associated with a model in terms of which the observed densities are interpreted. ρ_m consists of a Gaussian density centred on each atomic centre, and a floating background level. Interactions due to overlapping densities of neighbouring atoms are allowed for and the model is normally treated as a flexible chain so that bond lengths are conserved during movement. Alternatively, the atoms may be allowed to move independently. Site occupations and atomic radii are also refinable. The calculation is organized in terms of a 'molten zone' of up to ten residues, which moves along the chain one residue at a time, linear or non-linear constraints being applied to preserve chain continuity at each end of the zone. Provision is made for the zone to become active or inactive in predetermined regions of the molecule. A difference map $(\rho_o - \rho_m)$ is available at the end of the calculation, as is a molecular listing with revised coordinates and dihedral and inter-bond angles. Inter-bond angles may be treated either as constants or as variables, and if variable may be made elastically stiffer than dihedral angles.

The procedure is well suited to maps of 2 to 3 Å resolution, but is not limited to this range. It has produced convergent shifts exceeding 1.5 Å in a map of 2 Å resolution, and, except for shifts exceeding 1 Å, convergence is essentially complete in one pass. The procedure has, so far, been applied to four proteins.

Notation		
A, B	orthogonal matrices	G₂ projector matrix, equation (29)
a_i	atomic radius	$G(a, r)$ spherical Gaussian density, radius a , equation (1)
a_{ij}	compounded radius of two atoms, $a_{ij} = \sqrt{a_i^2 + a_j^2}$, $a_{ii} = a_i \sqrt{2}$	$g(a, x)$ one-dimensional Gaussian density, width a
B	temperature factor, isotropic	K scale factor
c	correlation coefficient	m normal matrix element, or an integer
D	rectangular matrix of derivatives	N number of grid points
D₁	rectangular matrix of $\frac{\partial \rho_m}{\partial x}$ values	n spindle vector, <i>i.e.</i> a vector joining two points in the structure about which part of the structure is allowed to rotate relative to the remainder
D₂	rectangular matrix of $\frac{\partial x}{\partial \theta}$ values	n̂ a spindle vector of unit length
d	background level	P rectangular matrix of eigenvectors defining a permitted subspace
E	W D U ⁻¹ , transformed derivative matrix	p, q general parameters, also subscripts 1, 2, 3 denoting components of a vector
E₁ & E₂	E matrices given by equation 20	R_1 & R_2 residuals [equations (5) and (56)]
E	F summed over grid points	r position vector in real space, (Å)
F	rectangular matrix of eigenvectors defining a forbidden subspace	r $ \mathbf{r} $
F	continuous function of position equal to $\rho_o \frac{\partial \rho_m}{\partial p}$	\mathbf{r}_{0i} $\mathbf{r} - \mathbf{r}_i$
F_o	observed structure factor, complex	r_{0i} $ \mathbf{r} - \mathbf{r}_i $
F_c or F_m	calculated structure factor based on ρ_m	\mathbf{r}_i Cartesian position vector of atom i
F_m^-	calculated structure factor based on ρ_m^-	\mathbf{r}_{ij} $\mathbf{r}_i - \mathbf{r}_j$
F_d	calculated structure factor based on background term alone	r_{ij} $ \mathbf{r}_{ij} $
f	effective atomic scattering factor	\mathbf{r}_γ Cartesian position vector of a grid point
		$\mathbf{r}_{\gamma i}$ $\mathbf{r}_\gamma - \mathbf{r}_i$
		$r_{\gamma i}$ $ \mathbf{r}_{\gamma i} $
		s position vector in reciprocal space, (Å ⁻¹); also column vector of wanted translations
		s_p p th component of s (reciprocal space)
		s $ \mathbf{s} $ (reciprocal space)
		$T(F)$ Fourier transform of F

t	column matrix of translations expressible in terms of conformational changes
U	square matrix such that $\bar{U}U$ contains parametric weights, usually diagonal
u	column matrix of residual translations
V	square matrix such that $\bar{V}V$ contains weights associated with translations
V	unit-cell volume
v	volume associated with each grid point in ρ_o map
dv	element of volume
W	square matrix such that $\bar{W}W$ are the observational weights, usually diagonal
x	column matrix of parametric quantities
x	Cartesian coordinate, (\AA)
x_{ip}	p th Cartesian component of r_i
x_{ijp}	p th Cartesian component of r_{ij}
x_{yp}	p th component of r_y
x_{ytp}	p th component of r_{yt}
y	column matrix of observational quantities
Z	filter matrix, square, having 0 or 1 in diagonal positions, zero elsewhere
Z_i	number of electrons in atom i
z	weighted parameters
δ_{pq}	Kronecker delta
ε	column matrix of observational residuals
θ	column matrix of adjustments to conformational angles, also the vector $\theta\hat{n}$
θ	Bragg angle or a conformational angle
Λ	matrix of eigenvalues, diagonal
A	lattice of δ -functions at grid points
λ_i	eigenvalues
λ	wavelength
μ	column matrix of eigenshifts
ϱ	column matrix comprising a list of ϱ values
ϱ	$\varrho_o - \varrho_m$
ϱ_o	observed electron density
$\varrho_{o\gamma}$	ϱ_o at a grid point
ϱ_m	model electron density
ϱ_m	that part of ϱ_m attributable to a single atom
ϱ_m	ϱ_m omitting the background term
Φ	column matrix of weighted conformational changes, $U\theta$
Ψ	column matrix of reduced conformational changes, equation (44)

1. Introduction

The purpose of the work described in this paper is to provide a reliable procedure for dealing with the quantitative aspects of the interpretation of an electron density map of a protein. It is in no way concerned with the qualitative aspects of interpretation and it is assumed at the outset that the preliminary interpretation of the map made by the crystallographer is essentially correct. The procedure does not experiment with alternatives, and a peptide link which is initially upside down, for example, will not be turned over unless this change is associated with a monotonically

decreasing residual. The procedure normally treats the protein as a flexible chain of linked atoms whose internal geometry is fixed except for specified flexibilities, and it normally operates in conditions where individual atoms are not resolved. For both these reasons it is necessary that the preliminary interpretation be satisfactory in its fixed geometry (such as bond lengths and the majority of inter-bond angles) and it is therefore essential that the trial structure should itself consist of the results of a mathematical model-building procedure such as those of Diamond (1966) or of Levitt & Lifson (1969). For the former it is not necessary to provide hand-measured coordinates for more than about three atoms per residue in order to generate a suitable trial structure for refinement, whilst the latter provides a minimum energy conformation.

In an earlier paper (Diamond, 1965), a study was made of the characteristics of flexible chains when these are refined against data in reciprocal space, whereas the present work uses data in real space. There are advantages and disadvantages to both, but it now seems clear that the balance of advantage lies with the real-space technique. Some of the relevant considerations are as follows:

(i) With the real-space procedure the number of derivatives which needs to be evaluated (independent atom model) is the product of the number of grid point densities affected by one atom and the number of atoms, n , which rises linearly on n for a given resolution. For the reciprocal-space technique the corresponding figure is the product of the number of atoms and the number of reflexions, which rises as n^2 for a given resolution. This alone would be sufficient reason for preferring real space for large molecules.

(ii) With the reciprocal-space technique it is always necessary, when considering each reflexion, to represent the whole of the molecule in some way even though only a part of it may be being refined. With the real-space technique, however, there is never more than the equivalent of ten residues of chain and the corresponding volume of density map present in the computer, so that there is no upper limit to the size of the molecule that may be refined. A large molecule takes longer, but has exactly the same core storage requirements as a small one. Ultimately, the limits are set by the length of a magnetic tape or the size of a disc storage device used for the electron densities.

(iii) Electron density maps of proteins commonly show signs of ordered material in the solvent interstices. Such effects can make close agreement between F_o and F_c values difficult to achieve, and in reciprocal-space refinement these effects cannot be separated from the protein diffraction. Contributions to ΔF arising from this source may perturb the refinement unless one can depend on their orthogonality to the derivatives of F with respect to the protein parameters, and this implies that a full set of data rather than a selection should be used. With the real-space technique solvent effects are naturally separated and do not affect the closeness

of fit which may be achieved between the observed and model densities within the protein.

(iv) The one respect in which the reciprocal-space technique appears to have an advantage, (at least in the final stages of refinement) is that it is possible there to weight the observations in accordance with their reliabilities, whereas it is assumed in the present work that the observed electron densities at all grid points are equally reliable. This is probably not true, especially near special positions and heavy atom sites. The question of observational weights, and the relationship of the adopted scheme to reciprocal-space weighting schemes is considered further below.

(v) Finally, the two techniques differ in that reciprocal-space techniques may be arranged to refine either against $|F_o|$ or against $|F_o| \exp \{i\alpha_o\}$ or $|F_o| \exp \{i\alpha_o\}$, using isomorphous replacement phases in the last case. Real-space refinement, on the other hand, implies that whatever phases were used in calculating the electron density are to be treated as observational quantities. This, too, may be counted a disadvantage of the real-space technique. However, phases derived from a previous cycle may be used to calculate the electron densities for the next.

The present work is a form of zone refinement. At any stage of the calculation there are represented in the computer a small number, < 10 , of consecutive amino acid residues. This zone is subdivided into two types of region. The greater part of it, normally, is called the molten zone. Atoms within the molten zone are generally free to move or to vary their weight and radius parameters. At each end of the zone there are margin regions within which the atoms are not permitted to move or vary their weight or radius. The margins serve two main purposes. One is to ensure that, by keeping them still, the chain remains at all times continuous with those parts of the chain which are not represented in the machine, and the other is concerned with the proper calculation of terms relating to atoms near the end of the molten zone for which overlap of density with neighbouring atoms must be allowed. For these atoms the neighbouring atoms may be in the margin. The margins may also be used for other special purposes, for example, it is possible to designate on the input listing that certain atom(s) shall at all times be treated as margin atoms even when they occur in the middle of the molten zone. This facility is particularly useful in pinning the far end of a cystine bridge when the calculation is following the course of the main chain, whilst still permitting most of the bridge to move. If this is not done, the far end of the bridge will be influenced by density in the map for which no corresponding atoms occur in the molecular listing at that point, whilst to include the distant main chain atoms in the listing leads to the need to deal with networks rather than chains with a single level of branching. Such bridges are normally represented twice, once in connexion with each portion of main chain to which they are attached. Both portions of

main chain are therefore free to move, but the two images of the bridge may fail to coincide exactly.

After each refinement (or group of refinements) the zone moves one residue along the chain, involving the output of one residue and the input of another. At the start and finish however, when a chain terminus is in the zone, a margin is only established at the end of the zone which adjoins the rest of the chain. Initially the zone is of zero length and several steps are required before it builds up to its assigned length, and there is a similar run-down stage at the end.

The structure which is being refined must be presented in the form of a list of atoms, main chain parameters and side chain parameters specifically ordered according to the rules set out by Diamond (1966) so that their order unambiguously indicates where branch points occur in the chain and where flexibility is to be introduced. All types of flexibility are treated *as if* they were dihedral angles, so that the introduction of a parameter between two atoms implies free rotation of the structure above this parameter in the list relative to the structure below it, about the line joining the two atoms concerned, with appropriate limitation on the range of action of side chain parameters. It is always the structure above a parameter which is moved by it, the structure below being stationary, so that the margin at the lower end (called the root end) of the zone can never move unless it contains a chain terminator which provides translational freedom of the chain terminus. On the other hand, every main chain parameter, if altered, moves the margin at the top of the zone and suitable constraint techniques are employed to maintain its position. (In this connexion the 'upper' and 'lower' ends of the zone relate to their positions on a page of printed output. The lower or root end contains structure most recently read into the zone and the upper end contains structure which is about to be output.) If it is required to introduce flexibility of another kind, inter-bond angles for example, this may be done by including suitably positioned dummy atoms in the listing, and inserting parameters between them. These atoms form an integral part of the chain and move as the chain moves, but they possess no electrons and have no direct influence on the refinement.

In order to economize in core storage requirements the electron density map is held on a disc or similar device, subdivided into pages containing up to 180 grid points each. As the molten zone moves along the molecule, those pages which are required are brought into core storage. Thus, for efficient working, it is only necessary for the core storage allocation to be sufficient to contain the density values within the molten zone, and may even be less. If it is less there is some loss of efficiency, and in some circumstances there may be a consequential systematic error, discussed below. Facilities are also provided which allow the map on the backing store device to completely span a whole molecule, with some to spare, even though only one asymmetric unit of densities need be provided originally

and the molecule may run into neighbouring asymmetric units.

2. The choice of model density and minimized residual

The assumed form of the model electron density is

$$\rho_m(\mathbf{r}) = K \sum_i Z_i G(a_i, \mathbf{r} - \mathbf{r}_i) + d \quad (1)$$

where

$$G(a, \mathbf{r}) = a^{-3} \exp \{-\pi r^2/a^2\}.$$

G is a spherical Gaussian function such that its volume integral is unity for all $a > 0$. a is thus an effective radius for an atom where its density is about one twentieth of its central value. Z_i is the number of electrons associated with atom i , K is an overall scale factor and d is a background level which, in principle, is $-F(000)/V$ if ρ_o is on an absolute scale and $F(000)$ is omitted, but in practice it varies slowly from place to place (see Fig. 1 and § 6). If the effective atomic scattering factor is written

$$f = Z \exp \{-B \sin^2 \theta/\lambda^2\}$$

then

$$a = \sqrt{B/4\pi}.$$

The choice of Gaussian form for the model atoms is largely arbitrary, but it would be difficult to argue that any particular alternative is necessarily superior. The function chosen for ρ_m has to be capable of representing an image of an isolated atom in the prevailing conditions which normally involve:

- (i) a low-resolution cut-off,
- (ii) a large experimental temperature factor,
- (iii) a fall-off of the figure of merit with increasing $\sin \theta/\lambda$.

Theoretically, therefore, the image of an isolated atom is the convolute of the true electron density distribution for an atom at rest with three other similar functions, and it is to be expected that this fourfold convolution will not be distinguishable from Gaussian to an extent which is worth characterizing. Although isolated atoms are uncommon in proteins (bound water molecules being the closest approach) one forms the impression from examining electron density maps at 2 to 3 Å resolution that their profiles vary within one map to an extent which makes it not worth while to seek a function which describes them more accurately and consistently than the Gaussian.

It is well known that the ratio of the gradient to the curvature of the electron density at a particular point gives an estimate of the vector distance from that point to the centre of the nearest peak of density, supposing the density in the peak to be quadratic in form. This fact has formed the basis of other methods of refinement in real space, as reviewed by Lipson & Cochran (1966) and by Cruickshank (1959). Such methods have been shown by Cochran (1951) to be equivalent to least-squares refinement with reciprocal-space data in

which f^{-1} is used as a weighting factor. Such procedures therefore give enhanced weight to high-angle reflexions which, in the context of protein crystallography, are generally the least-well phased. The real-space counterpart to this statement is to note that gradient/curvature techniques, at best, fit the maximum of the model density to the maximum of the observed density and are, therefore, essentially point-to-point fittings. As such, they suffer a number of disadvantages:

- (i) If a trial structure coordinate is far from the centre of an observed peak then writing (tensor notation)

$$x_i = \left(\frac{\partial^2 \rho}{\partial x_i \partial x_j} \right)^{-1} \frac{\partial \rho}{\partial x_j}, \quad (3)$$

which is valid only for quadratic ρ , gives a poor approximation to the shift vector x_i and may even diverge if the initial position lies on the fringe of the peak where the curvature of the density has opposite sign to that at the centre. If the observed density peak is Gaussian rather than quadratic an improvement is to write

$$\frac{x_i}{1 - 2\pi \bar{\mathbf{x}} \mathbf{A} \mathbf{x}} = \left(\frac{\partial^2 \rho}{\partial x_i \partial x_j} \right)^{-1} \frac{\partial \rho}{\partial x_j} \quad (4)$$

for density of the form $\exp \{-\pi \bar{\mathbf{x}} \mathbf{A} \mathbf{x}\}$ with \mathbf{A} positive definite, but even then, such a method must fail if the initial coordinate lies in the flat region outside the peak.

- (ii) They require the computation of $\partial \rho / \partial x_i$ and $\partial^2 \rho / \partial x_i \partial x_j$ at the initial position, which involves interpolation and differentiation in a table of ρ_o values which is usually very coarsely sampled, and the density gradient must be obtained accurately.

- (iii) If an observed electron density peak is skew, then fitting to its maximum does not necessarily provide the best fit over all.

Because of these considerations the chosen approach has been to aim to minimize a residual

$$R_1 = \int (\rho_o - \rho_m)^2 dv \quad (5)$$

and it is easy to show that

$$R_1 = \frac{1}{V} \sum |F_o - F_c|^2. \quad (6)$$

By choosing this approach we see that:

- (i) Equation (5) shows that we accomplish a volume fitting rather than point-to-point fitting, which seems preferable considering the strange shapes which commonly occur in protein maps.

- (ii) Equation (6) shows that the reciprocal space data are uniformly weighted, so that there is no enhanced dependence on those high-angle reflexions which are poorly phased.

- (iii) No interpolations are required. At no stage are the density or its derivatives at the atomic centre given any particular attention, all the fitting being done at the grid points where the observed electron densities are cited.

(iv) Because it is a volume fitting, the sums of products of derivatives which enter the normal matrices become volume integrals of functions of Gaussians, all of which are obtainable in closed form. Accordingly the normal matrices may be written down outright, rather than accumulated arithmetically.

(v) Allowance for overlap of unresolved atoms becomes a straightforward matter, although Cruickshank (1952) and Truter (1954) have shown that this can be done in gradient/curvature methods also.

(vi) Because it is a volume fitting convergence is to be expected provided that some part of the model density overlaps some part of the observed density. It is not necessary for the initial model coordinate to fall within the observed peak at all provided there is some overlap. Thus the convergence radius is of the order of 2 atomic radii, which is substantially more than can be achieved by gradient/curvature methods, and this is borne out in practice.

(vii) It suffers the penalty that it is usually necessary to involve the observed electron density at more than 100 grid points for each atom.

3. Volume integration

In order to minimise the residual R_1 we require the normal matrix elements $\frac{1}{v} \int \frac{\partial q_m}{\partial p} \frac{\partial q_m}{\partial q} dv$ and the column vector $\frac{1}{v} \int \frac{\partial q_m}{\partial p} (q_o - q_m) dv$ for parameters p and q . These integrals are analytic if p and q are any two of $K, d, a_i, Z_i, x_i, y_i, z_i, a_j, Z_j, x_j, y_j, z_j$ for atoms i and j except for those parts involving q_o . For these we note the grid sum

$$E = \sum_r \frac{\partial q_m}{\partial p} q_o \quad (7)$$

differs from the required integral by an amount which depends on the position of the atomic centre in relation to the grid points according to

$$E(\mathbf{r}_i) = \sum_r F(\mathbf{r}_r) = \int F(\mathbf{r}_i) A(\mathbf{r}) dv \quad (8)$$

writing F for $(\partial q_m / \partial p) q_o$ and A for a lattice of δ functions at the grid points $\mathbf{r} = \mathbf{r}_r$. This is evidently a convolution, so that the transform of $E(\mathbf{r}_i)$ exists only at points reciprocal to A . In particular, the origin term in reciprocal space is related to the constant part of $E(\mathbf{r}_i)$, *i.e.* to the required integral, and the remaining terms to its fluctuations.

Now, the transform of $(\partial q_m / \partial p) q_o$ is very similar to that of $(\partial q_m / \partial p) q'_m$ (unless p is K or d) so that the transform of the latter may be used to estimate the dependence of $E(\mathbf{r}_i)$ on \mathbf{r}_i . The result may be written

$$\frac{1}{v} \int \frac{\partial q_m}{\partial p} q_o dv = \sum_r \frac{\partial q_m}{\partial p} q_o - \frac{1}{v} \sum_{s \neq 0} T \left[\frac{\partial q_m}{\partial p} q'_m \right] \times \exp \{ -2\pi i \mathbf{r}_i \cdot \mathbf{s} \}. \quad (9)$$

This correction is good unless the definition is coarse and overlap is sufficient to make q_o substantially different from q'_m within the region where $\partial q_m / \partial p$ is substantial. This means that, ideally, the definition should be related to bond lengths (by a half or a third) rather than to the resolution, to sustain the accuracy of the correction.

We shall return to consider the detailed nature of these corrections in §§ 6 and 7. For the present we remark that if the ratio of an atomic radius, a , to the separation of grid points exceeds 2.5 then none of these corrections exceed $\frac{1}{2}\%$, but they become rapidly more severe as definition deteriorates. If the ratio mentioned is 2.0, some 7% corrections are involved, and at 1.2 the 'correction' may be many times larger than the grid sum itself. In practice, the terms in the summation in (9) are prearranged in order of increasing $|\mathbf{s}|$ and the summation is terminated when the exponential factor in $T(F)$ falls below 10^{-4} . The corrections are therefore made in low definition maps to the extent that they are needed, but time is not wasted on them if the definition is high. In any event, these corrections are made outside the inner loop which performs the \sum_r operation.

4. Filtering

Filtering plays an important part in what follows, especially § 8, so we shall review the main points before proceeding. For further discussion on this topic see, for example, Diamond (1958, 1965, 1966, 1969) and Scheringer (1968).

We begin by writing

$$\mathbf{y} = \mathbf{D}\mathbf{x} + \boldsymbol{\varepsilon} \quad (10)$$

in which the column matrix \mathbf{y} contains the observational quantities $y_{\text{obs}} - y_{\text{calc}}$ where y_{calc} is based on the starting values of the parameters, \mathbf{D} contains the derivatives $\partial y_{\text{calc}} / \partial x$, \mathbf{x} contains the parametric shifts which are to be calculated and $\boldsymbol{\varepsilon}$ contains the residuals. The quadratic of weighted residuals, $\boldsymbol{\varepsilon} \tilde{\mathbf{W}} \mathbf{W} \boldsymbol{\varepsilon}$, may then be minimized with respect to weighted parameters $\mathbf{z} = \mathbf{U}\mathbf{x}$ by setting

$$\mathbf{x} = \mathbf{U}^{-1}(\tilde{\mathbf{E}}\mathbf{E})^{-1} \tilde{\mathbf{E}}\mathbf{W}\mathbf{y} \quad (11)$$

in which

$$\mathbf{E} = \mathbf{W}\mathbf{D}\mathbf{U}^{-1}. \quad (12)$$

The transformed normal matrix, $\tilde{\mathbf{E}}\mathbf{E}$, then has the property that its i th eigenvalue, λ_i , is given by

$$\lambda_i = \frac{\text{decrement in } \boldsymbol{\varepsilon} \tilde{\mathbf{W}} \mathbf{W} \boldsymbol{\varepsilon} \text{ due to } i\text{th eigenshift}}{\text{increment in } \mathbf{x} \tilde{\mathbf{U}} \mathbf{U} \mathbf{x} \text{ due to } i\text{th eigenshift}} \quad (13)$$

in so far as the linear relation (10) holds. This is shown in Appendix A. Filtering based on these eigenvalues may be accomplished by writing

$$\mathbf{x} = \mathbf{U}^{-1} \mathbf{A} \mathbf{Z} (\tilde{\mathbf{A}} \tilde{\mathbf{E}} \mathbf{E} \mathbf{A})^{-1} \tilde{\mathbf{A}} \tilde{\mathbf{E}} \mathbf{W} \mathbf{y} \quad (14)$$

in which \mathbf{A} is orthogonal such that its columns are the eigenvectors of $\tilde{\mathbf{E}}\mathbf{E}$ and the bracketed matrix is diagonal. \mathbf{Z} is the filter matrix having ones on the

diagonal in positions corresponding to eigenvalues above some chosen limit, and zeros elsewhere. The eigenshifts referred to in (13) are the elements of the column matrix

$$\boldsymbol{\mu} = \mathbf{Z}(\bar{\mathbf{A}}\bar{\mathbf{E}}\bar{\mathbf{E}}\bar{\mathbf{A}})^{-1}\bar{\mathbf{A}}\bar{\mathbf{E}}\bar{\mathbf{W}}\mathbf{y}. \quad (15)$$

Since the eigenshifts are uncorrelated, setting any of them to zero, as is done by \mathbf{Z} , does not affect the required values of the remaining ones. Filtering thus provides a means of ensuring that large disturbances to the trial structure, as measured by $\bar{\mathbf{x}}\bar{\mathbf{U}}\mathbf{U}\mathbf{x}$, will not occur if the resultant decrement in the residual $\bar{\boldsymbol{\varepsilon}}\bar{\mathbf{W}}\mathbf{W}\boldsymbol{\varepsilon}$ is judged too small to justify the disturbance.

The choice of matrices \mathbf{U} and \mathbf{W} is considered below, where appropriate. The choice of \mathbf{Z} , however, is with the user of this procedure who may specify the maximum number of eigenshifts to be included by \mathbf{Z} , or a minimum value of λ_i below which eigenshifts are to be excluded, or a minimum value of λ_i/λ_{\max} below which they are to be excluded. In principle, Hamilton's (1965) significance test may be invoked to determine whether or not the reduction in $\bar{\boldsymbol{\varepsilon}}\bar{\mathbf{W}}\mathbf{W}\boldsymbol{\varepsilon}$ occasioned by reducing the number of zeros on the diagonal of \mathbf{Z} is significant, since each zero on the diagonal of \mathbf{Z} ranks as one linear constraint on the solution \mathbf{x} . In practice, however, choosing \mathbf{Z} on the basis of (13) in which $\bar{\mathbf{x}}\bar{\mathbf{U}}\mathbf{U}\mathbf{x}$ is designed to represent a strain energy may be preferred. It is not uncommon for protein density maps to be deficient in detail to an extent that the crystallographer's interpretation of the map at certain points may reflect his judgement of the most probable solution, having regard to stereochemical knowledge and experience, rather than an unequivocal reading of an unambiguous map. In such cases filtering on a basis less formal than by Hamilton's criterion permits the crystallographer to ensure that gross disturbances to his interpretation do not take place in regions where he prefers to trust his judgement.

5. Factorization and the grouping of parameters

Equation (1) shows that the parameters available for refinement are K , d , a_i , Z_i , and r_i and there are also the conformational variables, θ_j , in terms of which the r_i may be expressed. Now $\partial q_m/\partial p$ is an even function of position with respect to an atomic centre if p is K , d , a_i or Z_i , but is an odd function if p is a positional coordinate. Hence the normal matrix elements $\frac{1}{v} \int \frac{\partial q_m}{\partial p} \frac{\partial q_m}{\partial q} dv$ vanish if either of p and q is a positional parameter and the other is not. We may therefore separate refinement of K , d , a_i and Z_i from the positional parameters and refine these separately. This operation is described in § 6.

An interesting situation then arises regarding the positional and conformational variables because the observational equations may now be factorized.

The observational equations (10) may now be written

$$\boldsymbol{\rho} = \mathbf{D}_1\mathbf{D}_2\boldsymbol{\theta} + \boldsymbol{\varepsilon} \quad (16)$$

where the column matrix $\boldsymbol{\rho} = \boldsymbol{\rho}_o - \boldsymbol{\rho}_{mb}$ replaces \mathbf{y} ($\boldsymbol{\rho}_o =$ observed density, $\boldsymbol{\rho}_{mb} =$ model density before refinement), there being one element of $\boldsymbol{\rho}$ for each grid point in the molten zone, $\boldsymbol{\varepsilon} = \boldsymbol{\varepsilon}_o - \boldsymbol{\varepsilon}_{ma}$ ($\boldsymbol{\varepsilon}_{ma} =$ model density after refinement), \mathbf{D}_1 is rectangular and contains the derivatives $\partial q_m/\partial x$ in which x is a Cartesian coordinate in ångström units for each atom, so that the number of columns of \mathbf{D}_1 is three times the number of atoms in the molten zone, \mathbf{D}_2 contains the derivatives $\partial x/\partial \theta$ and the column vector $\boldsymbol{\theta}$ contains the increments which are to be computed and added to the conformational angles.

In this form the product

$$\mathbf{t} = \mathbf{D}_2\boldsymbol{\theta} \quad (17)$$

represents the collection of vector translations which will be applied to the atoms (neglecting the curvature of their loci) and there is a number of reasons why it is advantageous to solve for these translations as an intermediary in obtaining $\boldsymbol{\theta}$. The true solution to (16) is obtained when $\mathbf{W}\boldsymbol{\varepsilon}$ is orthogonal to every column of $\mathbf{W}\mathbf{D}_1\mathbf{D}_2$, i.e. when

$$\bar{\mathbf{D}}_2\bar{\mathbf{D}}_1\bar{\mathbf{W}}\mathbf{W}\boldsymbol{\varepsilon} = \mathbf{O} \quad (18)$$

and combination of (16) and (18) leads at once to (11) with \mathbf{E} now set equal to $\mathbf{W}\mathbf{D}_1\mathbf{D}_2\mathbf{U}^{-1}$ and $\boldsymbol{\theta}$ and $\boldsymbol{\rho}$ replacing \mathbf{x} and \mathbf{y} . Computationally this involves evaluating the derivative of q_m with respect to each θ at each grid point. This is difficult because several atoms in the vicinity of each grid point may enter into this relationship and all of these several atoms would need to be considered for each grid point and each parameter before moving on to the next unless \mathbf{D}_1 and \mathbf{D}_2 are evaluated separately and subsequently multiplied together. This would involve enormous storage requirements for \mathbf{D}_1 especially, and would not take full advantage of the fact that the elements of $\bar{\mathbf{D}}_1\mathbf{D}_1$ are analytic. Secondly, there might well arise circumstances in which it was desired to refine the coordinates as independent variables on a free-atom rather than a linked-atom basis. Thirdly, as will be set out in § 8, the procedures employed to conserve chain continuity by holding the margins still operate by fixing the coordinates of margin atoms. If the solution for $\boldsymbol{\theta}$ were obtained using the whole product $\mathbf{D}_1\mathbf{D}_2$ it would only be possible to aim at conserving chain continuity by ensuring that q_m does not alter in the margin region, and there would inevitably be difficulties in identifying which grid points, if any, have their density made up solely of contributions from margin atoms. Solution by way of wanted translations as intermediary therefore seems essential, and consequently we must consider the relationship between the two methods. The first method, using the complete product $\mathbf{D}_1\mathbf{D}_2$ we call method *A*, and the second, method *B*.

Reverting to equation (16) and introducing the observational weights \mathbf{W} and the weighted parameters $\boldsymbol{\phi} = \mathbf{U}\boldsymbol{\theta}$ we have

$$\mathbf{W}\boldsymbol{\varrho} = \mathbf{E}_1\mathbf{E}_2\boldsymbol{\varphi} + \mathbf{W}\boldsymbol{\varepsilon} \quad (19)$$

where

$$\begin{aligned} \mathbf{E}_1 &= \mathbf{W}\mathbf{D}_1\mathbf{V}^{-1} \\ \mathbf{E}_2 &= \mathbf{V}\mathbf{D}_2\mathbf{U}^{-1} \end{aligned} \quad (20)$$

in which \mathbf{V} is a weighting matrix on the translations which is analogous to \mathbf{U} and whose importance and character we now investigate. The best, but computationally difficult, solution is then

$$\boldsymbol{\theta}_A = \mathbf{U}^{-1}(\tilde{\mathbf{E}}_2\tilde{\mathbf{E}}_1\mathbf{E}_1\mathbf{E}_2)^{-1}\tilde{\mathbf{E}}_2\tilde{\mathbf{E}}_1\mathbf{W}\boldsymbol{\varrho}. \quad (21)$$

Alternatively, in method *B* we solve first for the translations \mathbf{s} ,* which would be required if the atoms were not linked, we have

$$\mathbf{W}\boldsymbol{\varrho} = \mathbf{W}\mathbf{D}_1\mathbf{s} + \mathbf{W}\boldsymbol{\varepsilon} \quad (22)$$

so that

$$\mathbf{s} = \mathbf{V}^{-1}(\tilde{\mathbf{E}}_1\mathbf{E}_1)^{-1}\tilde{\mathbf{E}}_1\mathbf{W}\boldsymbol{\varrho}. \quad (23)$$

This set of wanted translations, \mathbf{s} , may differ from any set \mathbf{t} which may be generated by rotations $\boldsymbol{\theta}$, so we write

$$\mathbf{s} = \mathbf{t} + \mathbf{u} \quad (24)$$

where \mathbf{u} is a residual set of translations which may be described as wanted but unavailable to a linked-atom model. We now solve (24) for $\boldsymbol{\theta}$ by minimizing $\tilde{\mathbf{u}}\tilde{\mathbf{V}}\mathbf{u}$, and obtain

$$\mathbf{V}\mathbf{s} = \mathbf{E}_2\mathbf{U}\boldsymbol{\theta} + \mathbf{V}\mathbf{u} \quad (25)$$

$$\boldsymbol{\theta}_B = \mathbf{U}^{-1}(\tilde{\mathbf{E}}_2\mathbf{E}_2)^{-1}\tilde{\mathbf{E}}_2\mathbf{V}\mathbf{s} \quad (26)$$

$$\boldsymbol{\theta}_B = \mathbf{U}^{-1}(\tilde{\mathbf{E}}_2\mathbf{E}_2)^{-1}\tilde{\mathbf{E}}_2(\tilde{\mathbf{E}}_1\mathbf{E}_1)^{-1}\tilde{\mathbf{E}}_1\mathbf{W}\boldsymbol{\varrho} \quad (27)$$

cf. equation (21).

$$\boldsymbol{\theta}_A = \mathbf{U}^{-1}(\tilde{\mathbf{E}}_2\tilde{\mathbf{E}}_1\mathbf{E}_1\mathbf{E}_2)^{-1}\tilde{\mathbf{E}}_2\tilde{\mathbf{E}}_1\mathbf{W}\boldsymbol{\varrho}.$$

We now enquire under what circumstances does $\boldsymbol{\theta}_A = \boldsymbol{\theta}_B$? It is not simply that \mathbf{u} must vanish. The two methods are equivalent if (18) is satisfied when $\boldsymbol{\theta}_B$ is inserted in (16), *i.e.* if

$$\begin{aligned} \tilde{\mathbf{D}}_2\tilde{\mathbf{D}}_1\tilde{\mathbf{W}}\mathbf{W} \cdot \boldsymbol{\varrho} &= \tilde{\mathbf{D}}_2\tilde{\mathbf{D}}_1\tilde{\mathbf{W}}\mathbf{W} \cdot \mathbf{D}_1\mathbf{D}_2 \\ &\cdot \mathbf{U}^{-1}(\tilde{\mathbf{E}}_2\mathbf{E}_2)^{-1}\tilde{\mathbf{E}}_2(\tilde{\mathbf{E}}_1\mathbf{E}_1)^{-1}\tilde{\mathbf{E}}_1\mathbf{W}\boldsymbol{\varrho} \end{aligned}$$

i.e. if

$$\tilde{\mathbf{U}}[\tilde{\mathbf{E}}_2\tilde{\mathbf{E}}_1 - \tilde{\mathbf{E}}_2\tilde{\mathbf{E}}_1\mathbf{E}_1\mathbf{E}_2(\tilde{\mathbf{E}}_2\mathbf{E}_2)^{-1}\tilde{\mathbf{E}}_2(\tilde{\mathbf{E}}_1\mathbf{E}_1)^{-1}\tilde{\mathbf{E}}_1]\mathbf{W}\boldsymbol{\varrho} = \mathbf{O} \quad (28)$$

i.e. if $\tilde{\mathbf{E}}_1\mathbf{E}_1$ commutes with $\mathbf{E}_2(\tilde{\mathbf{E}}_2\mathbf{E}_2)^{-1}\tilde{\mathbf{E}}_2$, for then the square bracket vanishes. Two matrices commute only if they are square and of the same order, as here, and have parallel eigenvectors. We define

$$\mathbf{G}_2 = \mathbf{E}_2(\tilde{\mathbf{E}}_2\mathbf{E}_2)^{-1}\tilde{\mathbf{E}}_2 \quad (29)$$

which is a projector matrix having the property that, [from (20) and (26)]

$$\mathbf{V}\mathbf{D}_2\boldsymbol{\theta}_B = \mathbf{V}\mathbf{t}_B = \mathbf{E}_2(\tilde{\mathbf{E}}_2\mathbf{E}_2)^{-1}\tilde{\mathbf{E}}_2\mathbf{V}\mathbf{s} = \mathbf{G}_2\mathbf{V}\mathbf{s} \quad (30)$$

thus it projects all possible sets of weighted wanted

translations, $\mathbf{V}\mathbf{s}$, onto the accessible set of weighted translations $\mathbf{V}\mathbf{t}_B$. All the eigenvalues of \mathbf{G}_2 are either zero or unity, the number of the latter being the number of conformational variables, θ , being varied (less the number of combinations of θ excluded by filtering, if any). Hence any orthonormal set of eigenvectors of \mathbf{G}_2 divides $\mathbf{V}\mathbf{s}$ space into two subspaces corresponding to $\lambda=0$ or, $\lambda=1$ respectively. Within each subspace the eigenvectors may be regarded as arbitrary except that they must be orthonormal. Thus for $\tilde{\mathbf{E}}_1\mathbf{E}_1$ to commute with \mathbf{G}_2 , every eigenvector of $\tilde{\mathbf{E}}_1\mathbf{E}_1$ must lie wholly in one subspace or wholly in the other. *i.e.* each eigenvector of $\tilde{\mathbf{E}}_1\mathbf{E}_1$ must either be expressible entirely as \mathbf{V} times a set of translations which can be generated by conformational variation, or it must be orthogonal to all such sets.

In practice it is not possible to ensure that this will be the case except by taking the following path. Let us define \mathbf{A} to be orthogonal such that

$$\tilde{\mathbf{A}}\tilde{\mathbf{D}}_1\tilde{\mathbf{W}}\mathbf{W}\mathbf{D}_1\mathbf{A} = \mathbf{A} \quad (31)$$

where \mathbf{A} is diagonal and set

$$\mathbf{V} = \mathbf{A}^{1/2}\tilde{\mathbf{A}}, \quad (32)$$

$\mathbf{A}^{1/2}$ also being diagonal. If we insert this value for \mathbf{V} into the expression for $\boldsymbol{\theta}_B$ we find that the expression for $\boldsymbol{\theta}_A$ results because $\tilde{\mathbf{E}}_1\mathbf{E}_1$ is then the identity and commutes with any \mathbf{G}_2 .

Operationally, we have already indicated the need to solve first for a vector of wanted translations and then to transmit this vector to a second procedure for conformational refinement, but we now have the alternatives of transmitting the vector \mathbf{s} or the vector $\mathbf{V}\mathbf{s}$ as either could form the interface between the two procedures. If $\mathbf{V}\mathbf{s}$ is chosen, then (23) and (32) yield

$$\mathbf{V}\mathbf{s} = \mathbf{A}^{-1/2}\tilde{\mathbf{A}}\tilde{\mathbf{D}}_1\tilde{\mathbf{W}}\mathbf{W}\boldsymbol{\varrho} \quad (33)$$

which (apart from a further factor $\mathbf{A}^{-1/2}$) are the eigenshifts for the translational refinement and are normally available, together with \mathbf{A} and $\tilde{\mathbf{A}}$. The following conformational refinement would then need to be based on equation (26), but since \mathbf{E}_2 contains \mathbf{V} it would also be necessary to transmit the matrix \mathbf{V} to the conformational refinement. Although this approach would permit the computation of $\boldsymbol{\theta}_A$ it is unfortunately rather impractical and cumbersome and loses many of the advantages of method *B*. Not only does a large volume of data need to be stored and transmitted from one procedure to the other, the computation of \mathbf{E}_2 would require storage for the whole of \mathbf{E}_2 and time to compute the product $\mathbf{V}\mathbf{D}_2$, and it would still be necessary to transform the constraints applicable to \mathbf{s} on the margin atoms to corresponding constraints applicable to $\mathbf{V}\mathbf{s}$.

If \mathbf{s} is transmitted in preference to $\mathbf{V}\mathbf{s}$, major simplifications are possible at the expense of computing only an approximation to $\boldsymbol{\theta}_A$. In the first place, substitution of (20) in (23) shows that \mathbf{s} is independent of \mathbf{V} provided \mathbf{V} is non-singular, so that, in this connexion, \mathbf{V} is

* This column vector \mathbf{s} has no connexion with the reciprocal-space vector \mathbf{s} of equation (9) and others derived therefrom.

important only in relation to the filtering of translational refinement where it is the quadratic $\tilde{\mathbf{V}}\mathbf{V}\mathbf{s}$ which is conserved. Secondly, substitution of (20) in (26) shows that the conformational refinement involves \mathbf{V} only through the product $\tilde{\mathbf{V}}\mathbf{V}$, which is not the case if $\mathbf{V}\mathbf{s}$ forms the given data, furthermore, since \mathbf{s} is independent of \mathbf{V} (except for the effect of filtering) it is not even essential that the \mathbf{V} used in calculating \mathbf{s} should be the same as the \mathbf{V} used in calculating $\boldsymbol{\theta}$ from \mathbf{s} .

Adopting (32) gives

$$\tilde{\mathbf{V}}\mathbf{V} = \tilde{\mathbf{D}}_1 \tilde{\mathbf{W}}\mathbf{W}\mathbf{D}_1 \quad (34)$$

and the approximation we shall adopt is to take only the diagonal elements of (34) for $\tilde{\mathbf{V}}\mathbf{V}$ when performing the conformational refinement. This means that we calculate a $\boldsymbol{\theta}$ as close to $\boldsymbol{\theta}_A$ as may be while maintaining all the computational advantages of method *B*. In effect it means that we allow fully for the effects of overlap between atoms when calculating the wanted translations, but in weighting these translations as data for the conformational refinement we simplify to a diagonal weighting scheme which accounts for the differing weights of the atoms but no longer carries an allowance for their overlap. Furthermore, since \mathbf{U} , \mathbf{V} and \mathbf{W} may all now be diagonal, calculation of \mathbf{E}_2 is no more trouble than calculation of \mathbf{D}_2 , and the calculation may be arranged so that it is never necessary to hold more than one (triple) row of \mathbf{E}_2 and the product $\tilde{\mathbf{E}}_2\mathbf{E}_2$. It is also the case that with this choice of \mathbf{V} the elements of $\tilde{\mathbf{V}}\mathbf{V}$ are analytic.

6. Refinement of scale factor, background, occupations and radii

In this section we outline the refinement of the parameters K , d , a_i and Z_i of equation (1). K is only refined if the Z_i are not refined.

The background level, d , is of little importance in itself but must be treated as a variable otherwise K , a_i and Z_i values would be in error and such errors must cause poor convergence or erratic results in the translational and conformational refinements. d values do vary considerably from place to place and there is evidence (Birktoft, private communication) that d is often more deeply negative in the interior of a molecule where ρ_0 is strongly modulated than it is near the molecular surface.

On the basis of equation (1) with all grid points given equal weight, *i.e.* $\mathbf{W}=\mathbf{I}$, there are then nine distinct types of normal matrix element of the form $\frac{1}{v} \int \frac{\partial \rho_m}{\partial p} \frac{\partial \rho_m}{\partial q} dv$ and these are derived in Appendix C and listed in Table 1.

Within this Table subscripts i and j refer to atoms and include the case $i=j$. Summations are over all atoms in the molten zone, not including the margins. N is the total number of grid points within the volume of the molten zone; its computation depends on the

way in which this volume is bounded, as described below.

Table 1. Normal matrix elements

p	q	$\frac{1}{v} \int \frac{\partial \rho_m}{\partial p} \frac{\partial \rho_m}{\partial q} dv$
K	K	$\frac{1}{v} \sum_i \sum_j Z_i Z_j G(a_{ij}, r_{ij})$
d	K	$\frac{1}{v} \sum_i Z_i$
d	d	N
a_i	K	$\frac{KZ_i a_i}{v} \sum_j \frac{Z_j}{a_{ij}^2} G(a_{ij}, r_{ij}) \left[2\pi \frac{r_{ij}^2}{a_{ij}^2} - 3 \right]$
a_i	d	0
a_i	a_j	$\frac{K^2 Z_i Z_j a_i a_j}{v a_{ij}^4} G(a_{ij}, r_{ij}) \left[4\pi^2 \frac{r_{ij}^4}{a_{ij}^4} - 20\pi \frac{r_{ij}^2}{a_{ij}^2} + 15 \right]$
Z_i	d	$\frac{K}{v}$
Z_i	a_j	$\frac{K^2 Z_i a_j}{v a_{ij}^2} G(a_{ij}, r_{ij}) \left[2\pi \frac{r_{ij}^2}{a_{ij}^2} - 3 \right]$
Z_i	Z_j	$\frac{K^2}{v} G(a_{ij}, r_{ij})$

Elements of the column vector $\tilde{\mathbf{D}}\tilde{\mathbf{W}}\mathbf{W}\boldsymbol{\rho}$ calculated according to the methods of § 3 are given in Table 2 and derived in Appendix D. In this table the subscript γ relates to an individual grid point, so that $\rho_{\gamma 0}$ is the observed density at that grid point and $r_{\gamma i}$ is its distance from the centre of atom i . i ranges over all atoms in the molten zone excluding the margins, but j ranges over the whole zone including the margins. This is because the j summations serve to subtract from ρ_0 the density ρ_m which is accounted for by the current parameter values, so that the vector $\boldsymbol{\rho} = \boldsymbol{\rho}_0 - \boldsymbol{\rho}_m$ contains only density which is accountable to adjustments within the molten zone. Note that summations over j are shown excluding the term $i=j$. This term does occur, but it is treated separately in connexion with the Fourier corrections to the grid sums.

The summations over \mathbf{s} are over a half-space excluding the origin with (hkl) and $(\bar{h}\bar{k}\bar{l})$ taken together in the following thirteen pairs: 3 of the form $\{100\}$, 6 of $\{110\}$ and 4 of $\{111\}$, arranged in order of increasing $|\mathbf{s}|$, these indices relating to the electron density grid as lattice. It is assumed that any Fourier terms involving higher indices are negligible, and if the definition of the map is so low that this is not the case then the corrections which are included are already so large as to be unreliable and a higher definition map should be used.

In Table 3 we show the results of a sample calculation of the corrections to be applied to the term for a_i on the basis of the assumptions that $d=0$, with a grid of side $l=\frac{1}{3}$ Å and with the atomic centre located exactly on a grid point or at a mesh centre midway

Table 2. Elements of the vector $\tilde{D}\tilde{W}\mathbf{w}_0$

$$\begin{aligned}
p & \sum_{\Gamma} \frac{\partial \rho_m}{\partial p} \rho_{o\gamma} - \frac{1}{v} \sum_{\mathbf{s}} T \left[\frac{\partial \rho_m}{\partial p} \rho'_m \right] \exp \{ -2\pi i \mathbf{r} \cdot \mathbf{s} \} \\
& - \frac{1}{v} \int \frac{\partial \rho_m}{\partial p} \rho_m \, dv \\
K & \sum_{\Gamma} \rho_{o\gamma} \sum_i Z_i G(a_i, r_{\gamma i}) \\
& - \frac{K}{v} \sum_i Z_i^2 G(a_{ii}, 0) \left[1 + 2 \sum_{\mathbf{s}} \exp \{ -\pi a_i^2 s^2 / 2 \} \cos 2\pi \mathbf{r}_i \cdot \mathbf{s} \right] \\
& - \frac{K}{v} \sum_{i \neq j} \sum_j Z_i Z_j G(a_{ij}, r_{ij}) \\
& - \frac{d}{v} \sum_i Z_i \left[1 + 2 \sum_{\mathbf{s}} \exp \{ -\pi a_i^2 s^2 \} \cos 2\pi \mathbf{r}_i \cdot \mathbf{s} \right] \\
d & \sum_{\Gamma} \rho_{o\gamma} - \frac{K}{v} \sum_i Z_i - Nd \\
a_i & K \sum_{\Gamma} \rho_{o\gamma} \frac{Z_i}{a_i} \left(2\pi \frac{r_{\gamma i}^2}{a_i^2} - 3 \right) G(a_i, r_{\gamma i}) \\
& + \frac{3K^2 Z_i^2}{2a_i v} G(a_{ii}, 0) \\
& \times \left[1 + 2 \sum_{\mathbf{s}} \left(1 + \frac{\pi a_i^2 s^2}{3} \right) \exp \{ -\pi a_i^2 s^2 / 2 \} \cos 2\pi \mathbf{r}_i \cdot \mathbf{s} \right] \\
& - \frac{K^2 Z_i a_i}{v} \sum_{j \neq i} \frac{Z_j G(a_{ij}, r_{ij})}{a_{ij}^2} \left(2\pi \frac{r_{ij}^2}{a_{ij}^2} - 3 \right) \\
& + \frac{4\pi K d Z_i a_i}{v} \sum_{\mathbf{s}} s^2 \exp \{ -\pi a_i^2 s^2 \} \cos 2\pi \mathbf{r}_i \cdot \mathbf{s} \\
Z_i & K \sum_{\Gamma} \rho_{o\gamma} G(a_i, r_{\gamma i}) \\
& - \frac{K^2 Z_i}{v} G(a_{ii}, 0) \left[1 + 2 \sum_{\mathbf{s}} \exp \{ -\pi a_i^2 s^2 / 2 \} \cos 2\pi \mathbf{r}_i \cdot \mathbf{s} \right] \\
& - \frac{K^2}{v} \sum_{j \neq i} Z_j G(a_{ij}, r_{ij}) \\
& - \frac{Kd}{v} \left[1 + 2 \sum_{\mathbf{s}} \exp \{ -\pi a_i^2 s^2 \} \cos 2\pi \mathbf{r}_i \cdot \mathbf{s} \right]
\end{aligned}$$

between eight adjacent grid points. In the Table, the figures for the corner are given to the left of those for the centre. The close agreement between the corrected

sum and the analytic integral in each case verifies the procedure and the figures for the correction illustrate the severity of the problem in low definition maps. The corresponding corrections for K and for Z_i are less severe than those for a_i . Typically, more than 90% of the time taken to evaluate an element of $\tilde{D}\tilde{W}\mathbf{w}_0$ is spent evaluating the grid sum, and less than 10% is spent on the j summation and Fourier corrections combined.

Computation of the vector element for d is quite seriously complicated by the effects of overlap. In the expression given in Table 2 for this element, $\sum_{\Gamma} \rho_{o\gamma}$

should be the sum of the observed densities attributable to atoms in the molten zone, $\sum Z_i$ should relate to the same atoms and N must be the number of grid points involved in forming the grid sum. Here, as for all other grid sums, we proceed from atom to atom and for each atom access every grid point which falls within a parallelepiped just large enough to contain a sphere of radius ca_i , where c is a chosen constant, $1 \leq c \leq 2$. This means that many grid points will be accessed several times, so that, in determining N , it is necessary to increment the count of grid points only the first time each grid point is accessed. For this reason the electron densities are stored as even integers and the least significant bit of each is used as a flag which is set to 1 the first time the grid point is accessed, and the count, N , is not increment on finding such a flag already set. This ensures that N corresponds to the volume occupied by the molten zone atoms, but $\sum_{\Gamma} \rho_{o\gamma}$ includes contributions from margin atoms which spill over into the volume of the molten zone and it is therefore necessary to subtract from $\sum_{\Gamma} \rho_{o\gamma}$ an estimate

of these contributions. This is done by considering each margin atom and accessing each grid point embraced by each such atom and at these grid points subtracting $KZ_i G(a_i, r_{\gamma i})$ from $\sum_{\Gamma} \rho_{o\gamma}$ only if the flag is

found to be set to 1. At the end of each cycle of refinement the flags are cleared.

The calculation is organized so that atoms are taken in the order in which they are listed, beginning at the end which has most recently entered the zone. If, in

Table 3. Examples of the application of Fourier corrections to the element for a_i

a (Å)	Corner		Centre		Corner		Centre	
a/l		0.4		0.8		1.2		1.2
$\frac{4\pi a^3}{3v}$		1.2		2.4		3.6		3.6
		7.2		57.8		195		195
Grid sum	-1760.6	+51.25	-35.129	-34.773	-6.9048	-6.9110	-6.9048	-6.9110
Calculated correction	+1208.0	-618.0	+0.174	-0.174	+8 × 10 ⁻⁶	-8 × 10 ⁻⁶	+8 × 10 ⁻⁶	-8 × 10 ⁻⁶
Corrected sum	-552.6	-566.75	-34.955	-34.947	-6.9048	-6.9110	-6.9048	-6.9110
Analytic integral		-559.33		-34.958		-6.9054		-6.9054
Residual, ϵ	+6.73	-7.42	+3 × 10 ⁻³	-11 × 10 ⁻³	+6 × 10 ⁻⁴	-56 × 10 ⁻⁴	+6 × 10 ⁻⁴	-56 × 10 ⁻⁴
Diagonal element, m , of normal matrix		3500		109		14.4		14.4
ϵ/m	+2 × 10 ⁻³	-2 × 10 ⁻³	+3 × 10 ⁻⁵	-1 × 10 ⁻⁴	+4 × 10 ⁻⁵	-4 × 10 ⁻⁴	+4 × 10 ⁻⁵	-4 × 10 ⁻⁴

proceeding along the list, the storage space allocated to the normal matrix is filled, then all subsequent atoms are treated as margin atoms overridingly.

The parametric weights, \mathbf{U} , for this refinement are set on a somewhat arbitrary basis, as follows. The normal matrix $\mathbf{D}\mathbf{W}\mathbf{W}\mathbf{D}$ is first calculated. \mathbf{U} is then taken to be diagonal and such that $\mathbf{E}\mathbf{E} = \mathbf{U}^{-1}\mathbf{D}\mathbf{W}\mathbf{W}\mathbf{D}\mathbf{U}^{-1}$ has unity in each diagonal position. $\mathbf{E}\mathbf{E}$ is then the correlation matrix and its mean eigenvalue is unity. This means that filtering based on its eigenvalues may readily include the more beneficial combinations of Z_i and a_i , which tend to be pair-wise correlated, whilst excluding those combinations which suffer from their high correlation simply by setting $\lambda_{\min} = 1$, thereby passing only the top half of the eigenvalue spectrum.

7. Translational refinement

This refinement determines the vector, \mathbf{s} , of wanted translations as discussed in § 5 using equation (23) transformed according to (14). For this purpose both \mathbf{V} and \mathbf{W} are identity matrices so that the grid point densities are again given equal weight and filtering conserves the sum of the squares of the wanted translations for real atoms, whatever their Z values. (A different \mathbf{V} is used in § 8).

All internal working is done in Cartesian coordinates in \AA . There is then only one type of normal matrix element given by

$$m_{ipjq} = \frac{1}{v} \int \frac{\partial \rho_m}{\partial x_{ip}} \frac{\partial \rho_m}{\partial x_{jq}} dv = \frac{2\pi K^2 Z_i Z_j G(a_{ij}, r_{ij})}{va_{ij}^2} \times \left[\delta_{pq} - 2\pi \frac{x_{ijp} x_{ija}}{a_{ij}^2} \right]. \quad (35)$$

Note that if $p \neq q$ the self-terms for $i=j$ vanish. Interaction elements between different atoms, $i \neq j$, generally exist if $p=q$, but if $p \neq q$ they are only important if the product $2\pi x_{ijp} x_{ija} / a_{ij}^2$ becomes large before $G(a_{ij}, r_{ij})$ has become small. The partial correlation coefficient

$$c_{ipjq} = \frac{m_{ipjq}}{\sqrt{m_{ipip} m_{jqjq}}} = \left(\frac{2a_i a_j}{a_{ij}^2} \right)^{5/2} 2\pi \frac{x_{ijp} x_{ija}}{a_{ij}^2} \times \exp \left\{ -\pi r_{ij}^2 / a_{ij}^2 \right\} \quad (36)$$

has maximum modulus $1/e$ which occurs when $a_i = a_j$ and \mathbf{r}_{ij} is along any of the $\langle 110 \rangle$ directions and of length $a_i \sqrt{2}/\pi$. In this case both correlations between atoms i and j involving the third axis vanish. Since the correlations between different coordinates of different atoms are limited and usually much less than the maximum, they have been ignored in order to obtain a ninefold saving of storage space. Ignoring elements with $p \neq q$ enables us to do three successive refinements for the three p values.*

* Techniques developed recently by Dr J. K. Reid of A.E.R.E. Harwell for diagonalizing band matrices offer the possibility of alleviating this situation.

The elements of the column vector $\mathbf{D}_1 \mathbf{W} \mathbf{W} \mathbf{e}$ are then, for coordinate p of atom i ,

$$\begin{aligned} & \frac{2\pi K Z_i}{a_i^2} \sum_{\mathbf{r}} x_{\gamma ip} \rho_{\sigma\gamma} G(a_i, r_{\gamma i}) \\ & + \frac{2\pi K Z_i}{v} \sum_{\mathbf{s}} [K Z_j G(a_{ij}, r_{ij}) \exp \{-\pi a_i^2 s^2 / 2\} \\ & + 2d \exp \{-\pi a_i^2 s^2\}] s_p \sin 2\pi \mathbf{r}_i \cdot \mathbf{s} \\ & - \frac{2\pi K^2 Z_i}{v} \sum_j \frac{Z_j x_{jip} G(a_{ij}, r_{ij})}{a_{ij}^2}. \end{aligned} \quad (37)$$

The summation over \mathbf{s} is over the same halfspace as in § 6 and the j summation again includes margin atoms. Matrix and vector elements for all three p values are assembled simultaneously.

In this refinement we proceed along the zone in the opposite direction from the procedure of § 6, *i.e.* we begin at the end which has been in the machine for the longest time. As before, if the normal matrix is filled before reaching the end of the zone all subsequent atoms are treated as margin atoms. This procedure ensures that in these circumstances all atoms which are processed for translational or conformational refinement have previously been processed for weight and radius refinement. This is probably beneficial for a structure in an advanced stage of refinement but in the early stages, when it is possible that some side chains may run out of density, it is questionable whether this idea has been a good one, as in such a case it would be possible for Z_i values to refine down to zero, after which no movement will occur, when a movement, if performed first, would let the side chain encounter some density. Control options exist, however, which permit the refinement of K and d without refining a or Z .

8. Conformational refinement

In this section we accept the column vector, \mathbf{s} , of wanted translations given by the methods of the previous section and determine the required conformational alterations from equation (26) and the diagonal of (34).

Each parameter in the structure is associated with a line joining two atoms in the structure, and these atoms may be either real or dummy. We call such a line a spindle vector. For any atom above a parameter in the list (after allowing for chain branching) the three elements of the matrix \mathbf{D}_2 are given by

$$\frac{\partial \mathbf{r}}{\partial \theta} = \hat{\mathbf{n}} \times \mathbf{r} \quad (38)$$

where $\hat{\mathbf{n}}$ is a unit spindle vector and \mathbf{r} is the position vector of the atom concerned relative to some point on the spindle. A diagonal \mathbf{U} matrix may conveniently be introduced at this point by setting

$$\text{elements of } \mathbf{D}_2 \mathbf{U}^{-1} = \mathbf{n} \times \mathbf{r} \quad (39)$$

in which the spindle now has

$$|n| = \text{diagonal element of } U^{-1}. \quad (40)$$

Any parameter which has its spindle set to zero at this stage will then behave as if it is perfectly rigid when filtering is employed. The larger $|n|$ is, the more elastically soft the parameter becomes, thus enabling filtering to provide a means of conserving elastic strain energies. Assigning small $|n|$ values to interbond angles and larger ones to dihedral angles alters the latter preferentially. All $|n|$ values are assignable, either implicitly or explicitly, by the user.

As already indicated in the introduction, it is necessary to introduce constraints to prevent margin atoms from moving. This is done by means of a subspace section, rather than by Lagrange multipliers, as follows.

First we scan the zone for margin atoms, for each of which we determine a triple row of E_2 [equations (20) and (39)] with V diagonal containing 1 for a margin atom (including dummy atoms) and zero for an atom in the molten zone. The matrix $\tilde{E}_2 E_2$ is accumulated without holding E_2 . $\tilde{E}_2 E_2$ is then diagonalized by an orthogonal A to give

$$A = \tilde{A} \tilde{E}_2 E_2 A. \quad (41)$$

Then, by (13), any eigenvector (column of A) with vanishing eigenvalue would produce no decrement in weighted residual, $\tilde{u} \tilde{V} V u$, for finite increment in $\tilde{\theta} \tilde{U} U \theta$ if a refinement were being conducted which sought to adjust margin atom coordinates. It follows that eigenvectors with $\lambda > 0$ correspond to combinations of rotations which, if applied, disturb the margins, but those having $\lambda = 0$ represent combinations of rotations which leave the margins unmoved. Clearly, any movements which are applied to the molten zone must be expressible as a linear combination of these latter eigenvectors. A may thus be partitioned:

$$A = (F|P) \quad (42)$$

in which F contains the forbidden eigenvectors having $\lambda > 0$ and P contains the permitted ones with $\lambda = 0$.

The methods used for finding A are those of Householder & Bauer (1959), Ortega (1960) and Wilkinson (1958, 1960) and these procedures fail to deliver orthonormal eigenvectors for coincident eigenvalues, so that F is determinate but P is not. However, the detailed nature of P is unimportant provided A is orthogonal. Therefore a valid P may be generated using the Gram-Schmidt process* against F .

Solving then for the weighted rotations $\varphi = U\theta$ we have from (25)

$$V s = E_2 \varphi + V u \quad (43)$$

in which E_2 now relates to real atoms in the molten zone using the diagonal of (34) for V , and in which we

may now write

$$\varphi = P \psi \quad (44)$$

and solve for ψ as unknowns. It is important that the same parametric weights, U , be used in (43) as were used when P was being established, but we are free to vary the weighting scheme, V , as we have done. Then (43) becomes

$$V s = E_2 P \psi + V u \quad (45)$$

hence

$$\tilde{P} \tilde{E}_2 V s = \tilde{P} \tilde{E}_2 E_2 P \psi \quad (46)$$

which, when diagonalized by an orthogonal B and filtered gives

$$\psi = B Z (\tilde{B} \tilde{P} \tilde{E}_2 E_2 P B)^{-1} \tilde{B} \tilde{P} \tilde{E}_2 V s \quad (47)$$

$$\theta = U^{-1} P B Z (\tilde{B} \tilde{P} \tilde{E}_2 E_2 P B)^{-1} \tilde{B} \tilde{P} \tilde{E}_2 V s. \quad (48)$$

Here the eigenvalues in $\tilde{B} \tilde{P} \tilde{E}_2 E_2 P B$ relate the decrement in the weighted residual translations $\tilde{u} \tilde{V} V u$ to the increment in $\tilde{\psi} \psi$. But

$$\tilde{\theta} \tilde{U} U \theta = \tilde{\varphi} \varphi = \tilde{\psi} \tilde{P} P \psi = \tilde{\psi} \psi \quad (49)$$

thus (48) provides a solution for θ which is filtered on the required basis and constrained to leave the margin atoms undisturbed.

The final atomic positions are then obtained from

$$r = \sum_0^{\infty} r_m \quad (50)$$

where

$$r_m = \frac{1}{m} \theta \times r_{m-1} \quad (51)$$

in which r_0 is the initial position of an atom relative to an atom on the spindle and r is its final position relative to the same point with

$$\theta = \theta \hat{n}. \quad (52)$$

This procedure moves the atoms along arcs of circles and involves non-linear dependence of the final positions on the angles, so that, if $\sum_2^{\infty} r_m$ is not negligible, movement of margin atoms will occur despite the precautions taken against this. These second order movements of margin atoms may then be removed by a corrective refinement against the original coordinates of the margin atoms alone. This refinement has a normal matrix comparable with that in equation (41) and is also filtered so that movements are now confined to a revised subspace F ; revised because the main refinement step changes the conformation of the protein on which F depends. This corrective refinement produces weighted rotations of the form

$$U \theta' = F' \psi' \quad (53)$$

(in which the prime denotes this corrective step), so that

$$(\tilde{\theta} + \tilde{\theta}') \tilde{U} U (\theta + \theta') = \tilde{\theta} \tilde{U} U \theta + 2 \tilde{\theta} \tilde{U} U \theta' + \tilde{\theta}' \tilde{U} U \theta' \quad (54)$$

* In this procedure a series of arbitrary vectors are orthogonalized with respect to all columns of F and all previously found columns of P and normalized.

in which the second term is

$$2\bar{\psi}\bar{P}F'\psi' \simeq 0 \quad (55)$$

which would vanish exactly if the F' were unprimed, and the third term is second order. The effect of this corrective refinement on $\bar{u}\bar{V}V\bar{u}$ is also second order, but may be of either sign.

This corrective refinement is optional in the existing program and may reasonably be omitted if the expected translations are small. In the case of a 2 Å map in which the zone contained five peptides, of which two formed the margins (*i.e.* three peptide links and four side chains in the molten zone), omission of the corrective refinement produced discontinuities in the protein chain $\sim 10^{-2}$ Å when the root-mean-square (r.m.s.) movements were ~ 0.3 Å. Inclusion of the corrective step produced perfect chain continuity within the limitations of the word length of the computer.

At the beginning and ending of a peptide chain atypical circumstances arise. At the beginning, several movements of the zone are generally required before the free end of the protein chain enters the upper margin, and until this happens the tip of the chain is free to move. At the chain terminus the situation is more complicated because, for the last few movements of the zone, the lower margin is missing. The normal procedure here is to include a chain terminator which introduces three degrees of translational freedom, and to precede this with suitable dummy atoms and main chain parameters to provide three degrees of rotational freedom also. With this arrangement, the chain terminus may move when the lower margin has run off the end of the chain and the constraint procedure already described holds the upper margin stationary. In this connexion, the parametric weights for the three translational parameters need consideration, and here the considerations raised by Scheringer (1968) are relevant. Scheringer has studied filtering in relation to the convergence properties of refinements against reciprocal space data, and for this purpose used the weighted radius of gyration of the group moved by a parameter as the parametric weight (diagonal element of U). This arrangement conserves the sum of squares of distances moved by the atoms (weighted also according to their Z values) rather than a strain energy which is the objective here. However, the three translational degrees of freedom at the chain terminus have no strain energy associated with them, yet they must be weighted in such a way that the filter does not exclude them purely because they are of a different character from the other conformational variables. As an example, consider the refinement of a haem group, a disc-like collection of atoms some ten ångströms across. If this is treated as an independent chain with three degrees of translational freedom and three degrees of rotational freedom about its mid-point, and if these parameters are given unit weight, then unit displacement of the latter produces movements ~ 5 Å,

whereas unit displacement of the translational parameters produces movements of only 1 Å. In these circumstances eigenvalues associated with the translations are smaller than those due to rotations and filtering criteria chosen as suitable for the protein chain may then be unsuitable for the haem group, and act to suppress the translations. For this reason assignable parametric weights are provided for the translational parameters associated with the chain terminator.

9. Residuals

At the time of writing, the seemingly trivial problem of characterizing the residual after refinement is not satisfactorily solved. It is clear that we should aim to quote R_1 [equation (5)] suitably normalized. However, the difficulty is that q_m contains d , and whilst d is recomputed for each zone position there is no uniquely defined d value associated with each grid point. Calculation of the difference $q_o - q_m$ requires the use of a flag system as in § 6 and results in a difference map with steps in it where the d value changes with movement of the zone. Alternatively, one could obtain a residual R_2 , like R_1 , but minimized with respect to a single d value applicable to the refined volume

$$R_2 = \sum^N (q_o - q_m)^2 - \frac{1}{N} \left[\sum^N (q_o - q_m) \right]^2 \quad (56)$$

in which q_m is q_m with the background term omitted, but even this calculation requires flags which must be independent of those of § 6, so that R_2 cannot be accumulated as the refinement proceeds and can only be obtained subsequently as an independent operation.

A difference map $q_o - q_m$ is available without this complication and an index of the smoothness of this map would be valuable. Evidently

$$R_1 = \int (q_o - q_m - d)^2 dv = \frac{1}{v} \sum |F_o - F_m - F_d|^2 \quad (57)$$

where F_m is the transform of q_m and F_d is the transform of the slowly varying background and is only appreciable near the origin of reciprocal space. A plot of $\langle |F_o - F_m|^2 \rangle$ against $2 \sin \theta / \lambda$ then gives an indication of R_1 in the region where F_d is negligible, but such a plot would contain contributions from partially ordered solvent or from any parts of the molecule which have not been refined, and this would have to be allowed for. It is intended to investigate these residuals in both real and reciprocal space.

10. Examples

In this section we give one or two examples of a preliminary nature. More detailed accounts of actual refinements must await papers on the proteins concerned.

Fig. 1 illustrates the largest definitely significant movement which the program has produced. The example is the 12A tryptophan in myoglobin. The

Figure shows a near-central x section through the side chain in a map at 2 Å resolution. (The reflexions used in calculating this map were only those which could be phased by the multiple isomorphous replacement method.) The movement which has occurred consists primarily of a change in χ_1 from -180° to -154° [χ_1 is the dihedral angle in the $C\alpha-C\beta$ bond, see Edsall, Flory, Kendrew, Liquori, Nemethy, Ramachandran & Scheraga (1966 *a, b, c*)] and it involves a movement of 1.6 Å at the end of the side chain. This occurred in two passes, 1.1 Å on the first pass and 0.5 Å on the second, the zone length being such that each pass involved four refinements of the side chain position. Convergent shifts as large as 4 Å have been produced that are mathematically plausible, but these have occurred in very ill-defined regions of the map where one can have little confidence in this or any other interpretation. They serve only to show the distances that can be traversed by this technique in order to reach higher density.

The stability of the process is also good. For the first 19 residues of myoglobin, including the first two which are ill-resolved, a first pass produced an r.m.s. movement of 0.521 Å taken over all real atoms, and 0.226 Å taken over main chain atoms only. On a second pass the corresponding figures were 0.203 and 0.118 Å. These figures were obtained with refinement of K and d active, but without refining Z_i or a_i values, and with the corrective refinement (non-linear constraints) included. Translational and conformational refinements were both filtered to pass two decades of the eigenvalue spectra. Under these conditions a zone having four side chains and five peptide links (two of them margins) moves once every $1\frac{1}{2}$ minutes on an IBM 360/44 computer, *i.e.* a mean rate of 1.5 min per residue, each residue undergoing 4 cycles.

I should like to acknowledge the use of a subroutine for diagonalizing matrices written by D. W. Matula and obtained through the IBM Share library, and I am indebted to Drs J. C. Kendrew and H. C. Watson for the use of the myoglobin data.

APPENDIX A

Derivation of equation 13

Setting

$$\omega = \mathbf{W}\mathbf{y}, \quad \zeta = \mathbf{W}\boldsymbol{\varepsilon}, \quad \mathbf{z} = \mathbf{U}\mathbf{x} \quad (\text{A1})$$

transforms (10) to

$$\omega = \mathbf{E}\mathbf{z} + \zeta. \quad (\text{A2})$$

The residual $\boldsymbol{\varepsilon}^T \mathbf{W} \mathbf{W} \boldsymbol{\varepsilon} = \tilde{\zeta} \zeta$ is minimized when ζ is orthogonal to every column of \mathbf{E} , *i.e.* when

$$\tilde{\mathbf{E}}\zeta = \mathbf{0}. \quad (\text{A3})$$

Premultiplying (A2) by $\tilde{\mathbf{E}}$, using (A3), gives the normal equations

$$\tilde{\mathbf{E}}\omega = \tilde{\mathbf{E}}\mathbf{E}\mathbf{z}. \quad (\text{A4})$$

Let $\zeta = \zeta_0$ when \mathbf{z} is the solution, \mathbf{z}_0 , of (A4), then, at some position \mathbf{z} in \mathbf{z} space near \mathbf{z}_0 , we may write

$$\zeta = \zeta_0 + \delta\zeta \quad \mathbf{z} = \mathbf{z}_0 + \delta\mathbf{z} \quad (\text{A5})$$

and from (A2)

$$\delta\zeta = -\tilde{\mathbf{E}}\delta\mathbf{z}. \quad (\text{A6})$$

Thus the residual associated with the point \mathbf{z} is

$$\begin{aligned} \tilde{\zeta}\zeta &= (\tilde{\zeta}_0 + \delta\tilde{\zeta})(\zeta_0 + \delta\zeta) \\ &= \tilde{\zeta}_0\zeta_0 - \delta\tilde{\mathbf{z}}\tilde{\mathbf{E}}\zeta_0 - \tilde{\zeta}_0\mathbf{E}\delta\mathbf{z} + \delta\tilde{\mathbf{z}}\tilde{\mathbf{E}}\mathbf{E}\delta\mathbf{z} \end{aligned} \quad (\text{A7})$$

in which the second and third terms vanish by (A3). Hence, in \mathbf{z} space

$$\tilde{\zeta}\zeta - \zeta_0\zeta_0 = \delta\tilde{\mathbf{z}}\tilde{\mathbf{E}}\mathbf{E}\delta\mathbf{z} = \text{const.} \quad (\text{A8})$$

is a surface of constant residual.

Let $\tilde{\mathbf{E}}\mathbf{E}$ be diagonalized by an orthogonal \mathbf{A}

$$\tilde{\mathbf{A}}\tilde{\mathbf{E}}\mathbf{E}\mathbf{A} = \boldsymbol{\Lambda} \quad (\text{A9})$$

and with

$$\mathbf{z} = \mathbf{A}\boldsymbol{\mu} \quad (\text{A10})$$

(A8) becomes

$$\tilde{\zeta}\zeta - \zeta_0\zeta_0 = \delta\tilde{\boldsymbol{\mu}}\boldsymbol{\Lambda}\delta\boldsymbol{\mu}. \quad (\text{A11})$$

Here the elements of $\delta\boldsymbol{\mu}$ are components of $\delta\mathbf{z}$ in the directions of the eigenvectors of $\tilde{\mathbf{E}}\mathbf{E}$.

For a linear problem (*i.e.* equation (A2) exact for any magnitude of \mathbf{z}) these equations hold for large $\delta\mathbf{z}$, in particular, they hold when the point \mathbf{z} comes to the origin

$$\mathbf{z} = \mathbf{0}, \quad \delta\mathbf{z} = -\mathbf{z}_0, \quad \delta\boldsymbol{\mu} = -\boldsymbol{\mu} \quad (\text{A12})$$

in which case $\tilde{\zeta}\zeta - \zeta_0\zeta_0$ becomes the decrement in the residual during a cycle of refinement, and the elements of $\boldsymbol{\mu}_0$ are the eigenshifts.

Evidently the contribution of the i th eigenshift to the decrement in the residual is $\lambda_i\mu_{0i}^2$, by (A11). Likewise its contribution to the increment in

$$\bar{\mathbf{x}}\tilde{\mathbf{U}}\mathbf{U}\mathbf{x} = \bar{\mathbf{z}}\mathbf{z} = \bar{\boldsymbol{\mu}}\tilde{\mathbf{A}}\mathbf{A}\boldsymbol{\mu} = \bar{\boldsymbol{\mu}}\boldsymbol{\mu} \quad (\text{A13})$$

is μ_{0i}^2 . Equation (13) follows immediately.

APPENDIX B

Definitions and identities

We define a one-dimensional Gaussian as

$$g(a, x) = \frac{1}{a} \exp\{-\pi x^2/a^2\} \quad (\text{B1})$$

then the spherical Gaussian

$$G(a, r) = \frac{1}{a^3} \exp\{-\pi r^2/a^2\} = \int_{p=1}^3 g(a, x_p) \quad (\text{B2})$$

and

$$\int_{-\infty}^{\infty} G(a, r) dv = \int_{-\infty}^{\infty} g(a, x) dx = 1. \quad (\text{B3})$$

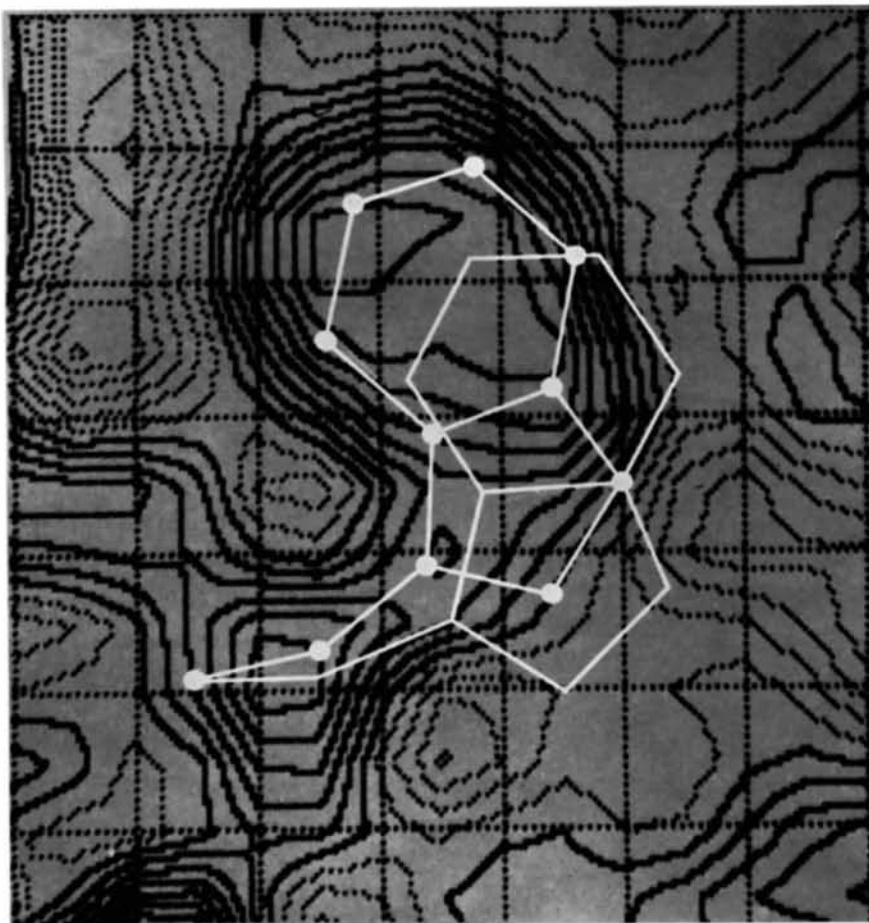


Fig. 1. A section at $x = 28/96$ of an electron density map of sperm whale myoglobin at 2 \AA resolution. The section is a nearly central section through tryptophan 12A and shows the movement of the side chain from its original position (unspotted) to a refined position (spotted) after two passes of the program. On a third pass a further movement of 0.1 \AA in the same direction occurred. All a_i values were fixed at 1.2 \AA . Section $x = 29$ shows substantially more density for atoms $C^{\beta 1}$ and $N^{\epsilon 1}$. The diagram was produced by the method of Gossling (1967). All contour spacings are equal, negative contours dotted.

We have then that

$$I_{2n} = \int_{-\infty}^{\infty} x^{2n} g(a, x) dx = \frac{(2n)!}{n!} \left(\frac{a^2}{4\pi}\right)^n \quad (B4)$$

$$I_{2n+1} = \int_{-\infty}^{\infty} x^{2n+1} g(a, x) dx = 0. \quad (B5)$$

(B4) may be obtained by successive integration by parts involving a recurrence relation between I_{2n} and I_{2n-2} .

Using the notation

$$x_{0k} = x - x_k, \quad x_{ij} = x_i - x_j \text{ etc. and } a_{ij} = \sqrt{a_i^2 + a_j^2}$$

it is easy to show that

$$g(a_i, x_{0i}) g(a_j, x_{0j}) = g\left(\frac{a_i a_j}{a_{ij}}, x_{0k}\right) g(a_{ij}, x_{ij}) \quad (B6)$$

in which

$$x_k = \frac{a_i^2 x_j + a_j^2 x_i}{a_{ij}^2} \quad (B7)$$

so that

$$\left. \begin{aligned} x_{ki} &= x_k - x_i = \frac{a_i^2 x_{ij}}{a_{ij}^2} \\ x_{kj} &= x_k - x_j = \frac{a_j^2 x_{ij}}{a_{ij}^2} \end{aligned} \right\} \quad (B8)$$

Then many of the required integrals are of the form

$$I_{n,m} = \int_{-\infty}^{\infty} x_{0i}^n x_{0j}^m g(a_i, x_{0i}) g(a_j, x_{0j}) dx. \quad (B9)$$

Replacing x_{0i} by $x_{0k} + x_{ki}$, using (B6) and the binomial theorem gives

$$I_{n,m} = g(a_{ij}, x_{ij}) \sum_{s=0}^n \sum_{t=0}^m \frac{n! m! x_{ki}^{n-s} x_{kj}^{m-t}}{s! (n-s)! t! (m-t)!} \times \int_{-\infty}^{\infty} x_{0k}^{s+t} g\left(\frac{a_i a_j}{a_{ij}}, x_{0k}\right) dx \quad (B10)$$

which, by (B4), (B5) and (B8) is

$$I_{n,m} = g(a_{ij}, x_{ij}) \sum_{\substack{s=0 \\ s+t \text{ even}}}^n \sum_{t=0}^m \frac{(-1)^{n-s} n! m! (s+t)! a_i^{2n-s+t} a_j^{2m+s-t}}{s! (n-s)! t! (m-t)! [(s+t)/2]! (4\pi)^{(s+t)/2} a_{ij}^{2n+2m-s-t}} \times x_{ij}^{n+m-s-t}. \quad (B11)$$

In particular

$$I_{0,0} = g(a_{ij}, x_{ij}) \quad (B12)$$

$$I_{1,0} = -g(a_{ij}, x_{ij}) \frac{a_i^2}{a_{ij}^2} x_{ij} \quad (B13)$$

$$I_{2,0} = g(a_{ij}, x_{ij}) \left[\frac{a_i^4 x_{ij}^2}{a_{ij}^4} + \frac{1}{2\pi} \left(\frac{a_i a_j}{a_{ij}}\right)^2 \right] \quad (B14)$$

$$I_{1,1} = g(a_{ij}, x_{ij}) \frac{1}{2\pi} \left(\frac{a_i a_j}{a_{ij}}\right)^2 \left[1 - 2\pi \frac{x_{ij}^2}{a_{ij}^2} \right] \quad (B15)$$

$$I_{2,2} = g(a_{ij}, x_{ij}) \left[\left(\frac{a_i a_j}{a_{ij}}\right)^4 \frac{x_{ij}^4}{a_{ij}^4} + \frac{1}{2\pi} \frac{a_i^4 - 4a_i^2 a_j^2 + a_j^4}{a_{ij}^2} \right. \\ \left. \times \left(\frac{a_i a_j}{a_{ij}}\right)^2 \frac{x_{ij}^2}{a_{ij}^2} + \frac{3}{4\pi^2} \left(\frac{a_i a_j}{a_{ij}}\right)^4 \right]. \quad (B16)$$

We shall also need

$$\int_{-\infty}^{\infty} \left(2\pi \frac{x_{0i}^2}{a_i^2} - 1\right) g(a_i, x_{0i}) g(a_j, x_{0j}) dx \quad (B17)$$

$$= \frac{2\pi}{a_i^2} I_{2,0} - I_{0,0} \\ = \frac{a_i^2}{a_{ij}^2} \left[2\pi \frac{x_{ij}^2}{a_{ij}^2} - 1 \right] g(a_{ij}, x_{ij}) \quad (B18)$$

and

$$\int_{-\infty}^{\infty} \left(2\pi \frac{x_{0i}^2}{a_i^2} - 1\right) \left(2\pi \frac{x_{0j}^2}{a_j^2} - 1\right) g(a_i, x_{0i}) g(a_j, x_{0j}) dx \quad (B19)$$

$$= \frac{4\pi^2}{a_i^2 a_j^2} I_{2,2} - \frac{2\pi}{a_j^2} I_{0,2} - \frac{2\pi}{a_i^2} I_{2,0} + I_{0,0} \quad (B20)$$

which similarly leads to

$$\frac{a_i^2 a_j^2}{a_{ij}^4} g(a_{ij}, x_{ij}) \left[4\pi^2 \frac{x_{ij}^4}{a_{ij}^4} - 12\pi \frac{x_{ij}^2}{a_{ij}^2} + 3 \right]. \quad (B21)$$

Some Fourier transforms will also be required. By expanding the complex exponential as a power series, and using (B4) and (B5) it is easy to show that

$$\int_{-\infty}^{\infty} g(a, x) \exp\{2\pi i x s\} dx \equiv T[g(a, x)] \\ = a^{-1} g(a^{-1}, s) \quad (B22)$$

$$\int_{-\infty}^{\infty} x g(a, x) \exp\{2\pi i x s\} dx \equiv T[xg(a, x)] \\ = i a s g(a^{-1}, s). \quad (B23)$$

Transforms involving higher powers of x may be obtained by noting that (B9) is a convolution, and hence

$$T[I_{m,n}(x_{ij})] = T^*[x_{0i}^m g(a_i, x_{0i})] T[x_{0j}^n g(a_j, x_{0j})] \quad (B24)$$

so that, for example

$$T[I_{1,1}(x_{ij})] = s^2 \frac{a_i^2 a_j^2}{a_{ij}} g(a_{ij}^{-1}, s) \quad (B25)$$

by (B6) and (B23), so that

$$T\left[\frac{1}{2\pi a_{ij}} \left(1 - 2\pi \frac{x_{ij}^2}{a_{ij}^2}\right) g(a_{ij}, x_{ij})\right] = s^2 g(a_{ij}^{-1}, s) \quad (B26)$$

by (B15), and conversely

$$T[x^2 g(a, x)] = \frac{a}{2\pi} (1 - 2\pi a^2 s^2) g(a^{-1}, s). \quad (B27)$$

Transforms of the form $T[x^{m+n}g(a, x)]$ may similarly be obtained in terms of those for x^m , x^n and lower powers.

APPENDIX C

Derivations of normal matrix elements in Table 1

We require first $\partial Q_m/\partial p$ for $p=K, d, a_i$ or Z_i at a general vector position \mathbf{r} and write $\mathbf{r}_{0i}=\mathbf{r}-\mathbf{r}_i$. All volume integrations are then over \mathbf{r} . Then from equation (1)

$$\frac{\partial Q_m}{\partial K} = \sum_i Z_i G(a_i, r_{0i}) \quad (C1)$$

$$\frac{\partial Q_m}{\partial d} = 1 \quad (C2)$$

$$\frac{\partial Q_m}{\partial a_i} = \frac{KZ_i}{a_i} G(a_i, r_{0i}) \left(2\pi \frac{r_{0i}^2}{a_i^2} - 3\right) \quad (C3)$$

$$\frac{\partial Q_m}{\partial Z_i} = KG(a_i, r_{0i}). \quad (C4)$$

(i) The K, K element is then, from (C1),

$$\frac{1}{v} \sum_i \sum_j Z_i Z_j \int G(a_i, r_{0i}) G(a_j, r_{0j}) dv \quad (C5)$$

which, when expanded by (B2) and (B12), gives

$$\frac{1}{v} \sum_i \sum_j Z_i Z_j G(a_{ij}, r_{ij}). \quad (C6)$$

(ii) The d, K element from (C1) and (C2) is

$$\frac{1}{v} \sum_i Z_i \int G(a_i, r_{0i}) dv = \frac{1}{v} \sum_i Z_i \quad (C7)$$

by (B3).

(iii) The d, d element, by (C2), is

$$\frac{V}{v} = N \quad (C8)$$

in which V is the volume over which the integration is taken and N is the number of grid points in this volume.

(iv) The a_i, K element, by (C1) and (C3), is

$$\frac{1}{v} \frac{KZ_i}{a_i} \int G(a_i, r_{0i}) \left(2\pi \frac{r_{0i}^2}{a_i^2} - 3\right) \sum_j Z_j G(a_j, r_{0j}) dv. \quad (C9)$$

Using (B2), gives

$$\begin{aligned} \frac{KZ_i}{va_i} \sum_j Z_j \iiint \sum_{p=1}^3 \left(2\pi \frac{x_{0ip}^2}{a_i^2} - 1\right) \\ \times \prod_{q=1}^3 g(a_i, x_{0iq}) g(a_j, x_{0jq}) dx_1 dx_2 dx_3 \end{aligned}$$

which, with (B12) and (B18), gives

$$\frac{KZ_i a_i}{v} \sum_j \frac{Z_j}{a_{ij}^2} \left(2\pi \frac{r_{ij}^2}{a_{ij}^2} - 3\right) G(a_{ij}, r_{ij}) \quad (C10)$$

(v) The a_i, d element, by (C2) and (C3), is

$$\frac{1}{v} \int \frac{\partial Q_m}{\partial a_i} dv$$

which must vanish because $\int Q_m dv$ is independent of a_i by (B3). Integration of (C3) using (B2) and (B4) confirms this.

(vi) The a_i, a_j element, by (C3), is

$$\frac{K^2 Z_i Z_j}{a_i a_j v} \int \left(2\pi \frac{r_{0i}^2}{a_i^2} - 3\right) \left(2\pi \frac{r_{0j}^2}{a_j^2} - 3\right) G(a_i, r_{0i}) G(a_j, r_{0j}) dv.$$

Using (B2) gives

$$\begin{aligned} \frac{K^2 Z_i Z_j}{a_i a_j v} \iiint \sum_{p=1}^3 \sum_{q=1}^3 \left(2\pi \frac{x_{0ip}^2}{a_i^2} - 1\right) \left(2\pi \frac{x_{0jq}^2}{a_j^2} - 1\right) \\ \times \prod_{s=1}^3 g(a_i, x_{0is}) g(a_j, x_{0js}) dx_1 dx_2 dx_3 \end{aligned}$$

which, with (B18) and (B21), becomes

$$\begin{aligned} \frac{K^2 Z_i Z_j}{a_i a_j v} G(a_{ij}, r_{ij}) \left[\sum_{p=1}^3 \sum_{q=1}^3 \frac{a_i^2 a_j^2}{a_{ij}^4} \left(2\pi \frac{x_{ijp}^2}{a_{ij}^2} - 1\right) \right. \\ \left. \times \left(2\pi \frac{x_{ijq}^2}{a_{ij}^2} - 1\right) + \sum_{p=1}^3 \frac{a_i^2 a_j^2}{a_{ij}^4} \left(4\pi^2 \frac{x_{ijp}^4}{a_{ij}^4} - 12\pi \frac{x_{ijp}^2}{a_{ij}^2} + 3\right) \right] \\ = \frac{K^2 Z_i Z_j a_i a_j}{a_{ij}^2 v} G(a_{ij}, r_{ij}) \left[4\pi^2 \frac{r_{ij}^4}{a_{ij}^4} - 20\pi \frac{r_{ij}^2}{a_{ij}^2} + 15 \right]. \end{aligned}$$

The remaining three elements in Table 1 have derivations closely modelled on those already given.

APPENDIX D

Derivations of the vector elements of Table 2

The expression to be evaluated for any parameter, p , is

$$\begin{aligned} \sum_{\mathbf{r}} \frac{\partial Q_m}{\partial p} \varrho_{o\mathbf{r}} - \frac{1}{v} \sum_{\mathbf{s}} T \left[\frac{\partial Q_m}{\partial p} \varrho'_{\mathbf{s}} \right] \exp \{-2\pi i \mathbf{r} \cdot \mathbf{s}\} \\ - \frac{1}{v} \int \frac{\partial Q_m}{\partial p} \varrho_m dv \quad (D1) \end{aligned}$$

in which T denotes Fourier transformation evaluated at those points in reciprocal space which form the lattice which is reciprocal to the grid on which the electron density is given, and $\varrho'_{\mathbf{s}}$ is that part of ϱ_m which depends on the parameter p , as described in § 3. The first term in this expression may be obtained directly from (C1–C4) without further discussion.

(i) For the K element the third term is

$$- \frac{1}{v} \int \sum_i Z_i G(a_i, r_{0i}) [K \sum_j Z_j G(a_j, r_{0j}) + d] dv \quad (D2)$$

in which the summation over i excludes the margins and the summation over j includes them. (D2) is

$$-\frac{K}{v} \sum_i \sum_j Z_i Z_j G(a_{ij}, r_{ij}) - \frac{d}{v} \sum_i Z_i \quad (\text{D3})$$

by (B2) and (B12).

To obtain the second term of (D1) we require, in principle, the transform of the integrand in (D2). As explained in the text, we approximate by replacing ϱ_m by ϱ'_m and ignore the effects of overlap for the purpose of estimating this correction. The correction is only large if the atoms are sharp peaks relative to the grid, and in these circumstances the overlap contributions for $i \neq j$ are likely to be small. Thus we require the Fourier transform of

$$K \sum_i Z_i^2 G^2(a_i, r_{0i}) + d \sum_i Z_i G(a_i, r_{0i}). \quad (\text{D4})$$

Now (B2) and (B6) give

$$G^2(a_i, r_{0i}) = G(a_{ii}, 0) G(a_i/\sqrt{2}, r_{0i}) \quad (\text{D5})$$

and

$$T[G(a_i, r_{0i})] = a_i^{-3} G(a_i^{-1}, s) \quad (\text{D6})$$

relative to atom i as origin, so that the transform of (D4) is

$$K \sum_i Z_i^2 G(a_{ii}, 0) \left(\frac{a_i}{\sqrt{2}}\right)^{-3} G(\sqrt{2}/a_i, s) + d \sum_i Z_i a_i^{-3} G(a_i^{-1}, s)$$

which is

$$K \sum_i Z_i^2 G(a_{ii}, 0) \exp\{-\pi a_i^2 s^2/2\} + d \sum_i Z_i \exp\{-\pi a_i^2 s^2\} \quad (\text{D7})$$

and the tabulated result follows.

(ii) The term for d is trivial to derive, but it is worth pointing out why it includes no Fourier correction term. This is because $\partial \varrho_m / \partial d$ is unity, hence the correction depends on $T(\varrho_m)$, or, better still, $T(\varrho_0)$ which is that part of F_0 attributable to the molten zone. Since its value is only required at points which are reciprocal to the electron density grid and since it is standard practice to subdivide the unit cell into at least three times the highest index used in computing ϱ_0 it follows that the reciprocal-lattice points required for the correction are at least three times further out than the furthest F_0 value used and the correction is therefore zero within the given context.

(iii) For the a_i element the third term in (D1) is

$$\frac{-1}{v} \int \frac{KZ_i}{a_i} \left(2\pi \frac{r_{0i}^2}{a_i^2} - 3\right) G(a_i, r_{0i}) \times [K \sum_j Z_j G(a_j, r_{0j}) + d] dv. \quad (\text{D8})$$

The part involving the j summation gives

$$\frac{-K^2 Z_i a_i}{v} \sum_j \frac{Z_j}{a_j^2} \left(2\pi \frac{r_{ij}^2}{a_j^2} - 3\right) G(a_{ij}, r_{ij}) \quad (\text{D9})$$

by comparison with (C9) and (C10), and the part involving d vanishes [see Appendix C § (v)].

For the Fourier correction we require the transform of the integrand in (D8) with $j=i$, i.e. of

$$\frac{K^2 Z_i^2}{a_i} \left(2\pi \frac{r_{0i}^2}{a_i^2} - 3\right) G^2(a_i, r_{0i}) + \frac{KZ_i d}{a_i} \left(2\pi \frac{r_{0i}^2}{a_i^2} - 3\right) G(a_i, r_{0i}). \quad (\text{D10})$$

Replacing $(2\pi r_{0i}^2/a_i^2 - 3)$ by $\sum_{p=1}^3 (2\pi x_{0ip}^2/a_i^2 - 1)$ and using (B2) and (B26) gives

$$-\frac{2\pi KZ_i ds^2}{a_i^2} G(a_i^{-1}, s) \quad (\text{D11})$$

for the second term in (D10), whilst the first term may be similarly treated on replacing $(2\pi r_{0i}^2/a_i^2 - 3)G^2(a_i, r_{0i})$ by

$$\frac{1}{2} G(2b, 0) \left[\left(2\pi \frac{r_{0i}^2}{b^2} - 3\right) - 3 \right] G(b, r_{0i}) \quad b = a_i/\sqrt{2}$$

leading to the tabulated correction.

(iv) The derivations for Z_i closely follow those for K .

APPENDIX E

Derivations for translational refinement

(i) Normal matrix elements.

The derivative with respect to the p th coordinate of atom i is

$$\frac{\partial \varrho_m}{\partial x_{ip}} = \frac{2\pi KZ_i x_{0ip}}{a_i^2} G(a_i, r_{0i}) \quad (\text{E1})$$

and is positive for $x_{0p} > x_{ip}$ because ϱ_m at a grid point rises if the atom moves towards it, having opposite sign to the gradient of ϱ_m at such a point. The required matrix element is then

$$\frac{4\pi^2 K^2 Z_i Z_j}{a_i^2 a_j^2 v} \int x_{0ip} x_{0jq} G(a_i, r_{0i}) G(a_j, r_{0j}) dv. \quad (\text{E2})$$

If $p = q$, (B2), (B3), (B6) and (B15) give

$$\frac{2\pi K^2 Z_i Z_j}{a_{ij}^2 v} \left(1 - 2\pi \frac{x_{ij}^2}{a_{ij}^2}\right) G(a_{ij}, r_{ij}) \quad (\text{E3})$$

whereas if $p \neq q$, (B2), (B3), (B6) and (B13) give

$$\frac{4\pi^2 K^2 Z_i Z_j}{a_i^2 a_j^2 v} \left(-\frac{a_i^2 x_{ijp}}{a_{ij}^2}\right) \left(-\frac{a_j^2 x_{ijq}}{a_{ij}^2}\right) G(a_{ij}, r_{ij}) \quad (\text{E4})$$

which, with (E3), simplifies to (35).

(ii) The element of the column vector $\bar{\mathbf{D}}_1 \bar{\mathbf{W}} \mathbf{W} \mathbf{Q}$ for x_{ip} is given by

$$\sum_r \frac{\partial \varrho_m}{\partial x_{ip}} \varrho_{or} - \frac{1}{v} \sum_s T \left[\frac{\partial \varrho_m}{\partial x_{ip}} \varrho'_m \right] \exp\{-2\pi i \mathbf{r} \cdot \mathbf{s}\} - \frac{1}{v} \int \frac{\partial \varrho_m}{\partial x_{ip}} \varrho_m dv. \quad (\text{E5})$$

The first term immediately gives

$$\frac{2\pi KZ_i}{a_i^2} \sum_{\Gamma} x_{\gamma i p} \rho_{0\gamma} G(a_i, r_{\gamma i}) \quad (\text{E6})$$

whilst the third is

$$-\frac{1}{v} \int \frac{2\pi KZ_i}{a_i^2} x_{0i p} G(a_i, r_{0i}) \times \left[\sum_{\Gamma} KZ_j G(a_j, r_{0j}) + d \right] dv \quad (\text{E7})$$

in which the term involving d vanishes and the other part gives

$$\frac{2\pi K^2 Z_i}{v} \sum_{\Gamma} Z_j \frac{x_{ij p}}{a_{ij}^2} G(a_{ij}, r_{ij}) \quad (\text{E8})$$

by (B2) and (B13).

The Fourier correction is the transform of

$$\frac{2\pi KZ_i x_{0i p}}{a_i^2} G(a_i, r_{0i}) [KZ_j G(a_j, r_{0j}) + d] \quad (\text{E9})$$

in which the first part is

$$\frac{2\pi K^2 Z_i^2}{a_i^2} T[x_{0i p} G^2(a_i, r_{0i})] \quad (\text{E10})$$

which is

$$\frac{2\pi K^2 Z_i^2}{a_i^2} G(a_{ii}, 0) i_{s_p} \frac{\sqrt{2}}{a_i} G(\sqrt{2}/a_i, s) \quad (\text{E11})$$

by (B2), (B6), B(22) and (B23), so that the required transform is

$$\pi K^2 Z_i^2 G(a_{ii}, 0) \times \sum_{\text{whole space}} i_{s_p} \exp \{ -\pi a_i^2 s^2 / 2 \} \exp \{ -2\pi i \mathbf{r}_i \cdot \mathbf{s} \} \quad (\text{E12})$$

$$= 2\pi K^2 Z_i^2 G(a_{ii}, 0) \times \sum_{1/2 \text{ space}} s_p \exp \{ -\pi a_i^2 s^2 / 2 \} \sin 2\pi \mathbf{r}_i \cdot \mathbf{s} \quad (\text{E13})$$

which enters (E5) with a sign reversal, to give (37), because (8) involves $F(\mathbf{r}_{0i})$, not $F(\mathbf{r}_{i0})$. The second part of (E9) similarly gives

$$4\pi K d Z_i \sum_{1/2 \text{ space}} s_p \exp \{ -\pi a_i^2 s^2 \} \sin 2\pi \mathbf{r}_i \cdot \mathbf{s} \quad (\text{E14})$$

References

- COCHRAN, W. (1951). *Acta Cryst.* **4**, 408.
 CRUICKSHANK, D. W. J. (1952). *Acta Cryst.* **5**, 511.
 CRUICKSHANK, D. W. J. (1959). *International Tables for X-ray Crystallography*, Vol. II. Birmingham: Kynoch Press.
 DIAMOND, R. (1958). *Acta Cryst.* **11**, 129.
 DIAMOND, R. (1965). *Acta Cryst.* **19**, 774.
 DIAMOND, R. (1966). *Acta Cryst.* **21**, 253.
 DIAMOND, R. (1969). *Acta Cryst.* **B25**, 805.
 EDSALL, J. T., FLORY, P. J., KENDREW, J. C., LIQUORI, A. M., NEMETHY, G., RAMACHANDRAN, G. N. & SCHERAGA, H. A. (1966a). *J. Biol. Chem.* **241**, 1004.
 EDSALL, J. T., FLORY, P. J., KENDREW, J. C., LIQUORI, A. M., NEMETHY, G., RAMACHANDRAN, G. N. & SCHLERAGA, H. A. (1966b). *Biopolymers*, **4**, 130.
 EDSALL, J. T., FLORY, P. J., KENDREW, J. C., LIQUORI, A. M., NEMETHY, G., RAMACHANDRAN, G. N. & SCHERAGA, H. A. (1966c). *J. Mol. Biol.* **15**, 339.
 GOSSLING, T. H. (1967). *Acta Cryst.* **22**, 465.
 HAMILTON, W. C. (1965). *Acta Cryst.* **18**, 502.
 HOUSEHOLDER, A. S. & BAUER, F. L. (1959). *Numerische Mathematik* 1. Band 1. Heft, S. 29.
 LEVITT, M. & LIFSON, S. (1969). *J. Mol. Biol.* **46**, 269.
 LIPSON, H. & COCHRAN, W. (1966). *The Determination of Crystal Structures*. London: Bell.
 ORTEGA, J. M. (1960). *J. Assoc. Computing Machinery*, **7**, 260.
 SCHERINGER, C. (1968). *Acta Cryst.* **B24**, 947.
 TRUTER, M. R. (1954). *Acta Cryst.* **7**, 73.
 WILKINSON, J. H. (1958). *Comp. J.* **1**, 90.
 WILKINSON, J. H. (1960). *Comp. J.* **3**, 23.

Acta Cryst. (1971). **A27**, 452

Accelerated Convergence of Crystal-Lattice Potential Sums*

BY DONALD E. WILLIAMS

Department of Chemistry, University of Louisville, Louisville, Kentucky, U.S.A.

(Received 28 September 1970)

A method for increasing the rate of convergence of general crystal lattice sums of the type $\sum_{j \neq k} q_j q_k r_{jk}^{-n}$ is described. The method is applicable for $n > 3$, or for $n > 0$ if $\sum_{\text{cell}} q_j = 0$. A numerical example is given for the London dispersion energy ($n=6$) of the benzene crystal. The calculation effort required to obtain the lattice sum was reduced at least tenfold.

Introduction

We consider here crystal lattice pairwise sums of the

type

$$S_n = \frac{1}{2} \sum_{j \neq k} q_j q_k r_{jk}^{-n},$$

for a general composite lattice. The subscript j runs over one unit cell, while the subscript k runs over the entire lattice, excepting $j=k$. The constants q_j are as-

* A preliminary account of this work was presented at the Eighth International Congress of Crystallography at Stony Brook, N.Y., August 1969.